

University of Alberta

Library Release Form

Name of Author: Negin Razavilar

Title of Thesis: Chromatographic Separation of Asphaltenes on Silica Materials

Degree: Master of Science

Year this Degree Granted: 2009

Permission is hereby granted to the University of Alberta Library to reproduce single copies of this thesis and to lend or sell such copies for private, scholarly or scientific research purposes only

The author reserves all other publication and other rights in association with the copyright in the thesis, and except as herein before provided, neither the thesis nor any substantial portion thereof may be printed or otherwise reproduced in any material form whatever without the author's prior written permission

Negin Razavilar

Date:30/09/2009

University of Alberta

Chromatographic Separation of Asphaltenes on Silica Materials

by

Negin Razavilar

A thesis submitted to the Faculty of Graduate Studies and Research
in partial fulfillment of the requirements for the degree of

Master of Science

Chemicals and Materials Engineering

© Negin Razavilar
Fall 2009
Edmonton, Alberta

Permission is hereby granted to the University of Alberta Libraries to reproduce single copies of this thesis and to lend or sell such copies for private, scholarly or scientific research purposes only. Where the thesis is converted to, or otherwise made available in digital form, the University of Alberta will advise potential users of the thesis of these terms.

The author reserves all other publication and other rights in association with the copyright in the thesis and, except as herein before provided, neither the thesis nor any substantial portion thereof may be printed or otherwise reproduced in any material form whatsoever without the author's prior written permission.

Examining Committee

Murray R.Gray, Chemical and Materials Engineering

Steven M.Kuznicki, Chemical and Materials Engineering

Mark McDermott, Chemistry, University of Alberta

ABSTRACT

In this study, we describe the use of different silica materials to separate vanadium compounds from Asphaltenes. We used high performance flash chromatography separation method to separate asphaltenes at different solvent strengths on sea sand. The separation conditions were optimized for flow rate and the strength of the solvent. The selectivity of separation was determined based on asphaltene and metal recovery. With separation on sea sand as the solvent strength increased, the recovery percentage of the asphaltenes also increased. Similarly, stronger solvent blends give poor selectivity based on peak shifts in fluorescence spectra. The separation conditions were then used to compare the performance of a series of silica materials treated with alkaline earth metals. These samples were treated with the same molar concentration of reactant at the same temperature. Treatment of silica materials resulted in an increase in metals recovery and asphaltene recovery by providing less active sites for adsorption.

ACKNOWLEDGMENT

I am deeply grateful to Dr.Murray Gray and Dr.Steven Kuznicki for guiding me as a graduate student to higher paths of knowledge.

Thanks for the funding provided by Imperial Oil and the valuable collaboration of Mrs. Andree Koenig , Tuyet Le and Kavithaa Loganathan along the project. Also, I would like to thank the entire faculty, administrative and technical staff of the University of Alberta for assisting me in acheiving my goals.

Finally my recognition to god and my lovely family for supporting and empowering me to be a better human being every day; to my wondrous friends from all over the world for showing me that friendship overcomes any difference in culture.

TABLE OF CONTENTS

CHAPTER 1 **1**

INTRODUCTION **1**

1.1 BACKGROUND **1**

1.2 RESEARCH APPROACH **4**

CHAPTER 2 **5**

LITERATURE REVIEW **5**

2.1 CHEMISTRY OF VANADIUM AND NICKEL IN BITUMEN **5**

2.1.1 CHEMISTRY OF VANADIUM IN BITUMEN **5**

2.1.2 CONCENTRATIONS OF METALS IN BITUMEN MATERIALS **7**

2.2 CHEMISTRY OF ASPHALTENES **7**

2.3 BASIS FOR ASPHALTENE COLOR **9**

2.4 SPECTROSCOPY OF ASPHALTENES **9**

2.4.1 UV-VISIBLE SPECTROSCOPY **10**

2.4.2 FLUORESCENCE SPECTROSCOPY OF ASPHALTENE SOLUTIONS **11**

2.5 AGGREGATION OF ASPHALTENE COMPONENTS **12**

2.6	SOLVENT FRACTIONATION OF ASPHALTENES	13
2.7	ADSORPTION OF ASPHALTENES TO SURFACES	14
2.7.1	REVERSIBILITY OF ASPHALTENE ADSORPTION	14
2.7.2	EFFECT OF ASPHALTENE AGGREGATION AND SOLUBILITY ON ADSORPTION	15
2.7.3	EFFECT OF SURFACE CHEMISTRY OF THE ADSORBENT	16
2.8	SILICA ADSORBENTS	18
2.8.1	SURFACE CHEMISTRY	18
2.8.1.1	Types of surface hydroxyl-groups	18
2.9	BASIC PRINCIPLES OF CHROMATOGRAPHY	20
2.10	REFERENCES	23
CHAPTER 3		28
MATERIALS AND METHODS		28
3.1	MATERIALS	28
3.2	EXPERIMENTAL PROCEDURE	29
3.2.1	CHROMATOGRAPHY PACKING PREPARATION	29
3.2.2	CHROMATOGRAPHY EXPERIMENTAL PROCEDURE	30
3.2.2.1	Open column chromatography	30
3.2.2.2	Flash chromatography using sea sand as chromatography packing	30
3.2.2.3	Scale up calculations for sea sand	31

3.2.2.4	Flash chromatography using modified silica materials as chromatography packing	33
3.2.3	EXPERIMENTS IN HEXANE/TOLUENE SOLUTION	34
3.2.3.1	Experiments performed at 50C	34
3.2.3.2	Experiments performed at room temperature	34
3.2.4	SOLVENT EVAPORATION	34
3.2.5	ACID DIGESTION	35
3.3	HIGH PERFORMANCE FLASH CHROMATOGRAPHY (HPFC)	35
3.4	ANALYTICAL METHODS	38
3.4.1	FT-IR SPECTROSCOPY	38
3.4.2	X-RAY PHOTOELECTRON SPECTROSCOPY (XPS)	38
3.4.3	FLUORESCENCE SPECTROSCOPY	39
3.4.4	INDUCTIVE COUPLED PLASMA SPECTROSCOPY	40
<u>CHAPTER 4</u>		<u>41</u>
<u>RESULTS & DISCUSSION OF SEPARATIONS ON SEA SAND</u>		<u>41</u>
4.1	SELECTION OF SOLVENT COMPOSITION FOR CHROMATOGRAPHY OF ASPHALTENES	41
4.2	DETERMINATION OF THE FLOCCULATION POINT OF ASPHALTENES FOR	
	CHROMATOGRAPHIC SEPARATION	41
4.3	RECOVERY OF COLD LAKE ASPHALTENES FROM SEA SAND	42

4.3.2	REPEATABILITY OF ASPHALTENE SEPARATION ON SEA SAND	45
4.4	EFFECT OF SOLVENT STRENGTH ON ASPHALTENE RECOVERY	46
4.5	FLUORESCENCE SPECTRA OF COLD LAKE ASPHALTENES SEPARATED ON SEA SAND	49
4.6	SEA SAND TREATED WITH ACID AND BASE	51
4.7	SEPARATION OF VANADIUM	54
4.7.1	REPEATABILITY OF VANADIUM SEPARATIONS ON SEA SAND	54
4.7.2	VANADIUM RECOVERY IN CHROMATOGRAPHIC FRACTIONS	55
4.8	EFFECT OF COLUMN TEMPERATURE	58
4.9	DISCUSSION	63
4.10	CONCLUSIONS	64
4.11	REFERENCES	65
CHAPTER 5		66
SEPARATION ON MODIFIED SILICA MATERIALS		66
5.1	INTRODUCTION	66
5.2	HYDROTHERMAL TREATMENT OF SILICA	66
5.3	RESULTS & DISCUSSION	68
5.3.1	RECOVERY OF COLD LAKE ASPHALTENES FROM DIFFERENT SILICA MATERIALS	68
5.3.2	METAL RECOVERY PERCENTAGE FROM DIFFERENT SILICA MATERIALS	68

5.3.3	SURFACE CHARACTERIZATION RESULTS	70
5.3.3.1	FTIR Spectroscopy results	70
5.3.3.2	XPS results	71
5.3.4	FLUORESCENCE SPECTRA OF COLD LAKE ASPHALTENES FROM TREATED SILICA MATERIALS	74
5.4	CONCLUSIONS	79
5.5	REFERENCES	81
<u>CHAPTER 6</u>		82
<u>GENERAL DISCUSSIONS & CONCLUSIONS</u>		82
<u>CHAPTER 7 APPENDIX A</u>		83
7.1	FTIR RESULTS FOR SURFACE CHARACTERIZATION	83
<u>CHAPTER 8 APPENDIX B</u>		88
8.1	HYDROTHERMAL PREPARATION OF SILICA MATERIALS	88
8.2	ASPHALTENE AND METAL RECOVERIES FOR DIFFERENT SILICA MATERIALS	88
<u>CHAPTER 9 APPENDIX C</u>		90
9.1	NI CONCENTRATIONS OBTAINED FROM ICP ANALYSIS	90

LIST OF FIGURES

FIGURE 2-1 PORPHINE-THE BASIC STRUCTURE OF PORPHYRINS, (SPEIGHT 2006)	6
FIGURE 2-2 AVERAGE MOLECULAR STRUCTURAL MODELS OF ASPHALTENE FRACTION OF PETROLEUM (SUZUKI 1982)	9
FIGURE 2-3 DESORPTION KINETICS OF FURRIAL ASPHALTENES FROM SILICA PLATE AT ROOM TEMPERATURE IN TOLUENE. (CASTILLO, FERNÁNDEZ ET AL. 2001)	15
FIGURE 2-4 SILANOL GROUPS ON SURFACE OF SILICA MATERIAL.....	16
FIGURE 2-5 DIFFERENT SILANOL GROUPS.....	20
FIGURE 2-6 SCHEMATIC OF COLUMN CHROMATOGRAPHY SETUP.....	21
FIGURE 3-1 HIGH PERFORMANCE FLASH CHROMATOGRAPHY ASSEMBLY	32
FIGURE 3-2 SP1—THE SINGLE-COLUMN FLASH PURIFICATION SYSTEM, IMAGE FROM BIOTAGE COMPANY WITH PERMISSION.	36
FIGURE 3-3 FLUORESCENCE SPECTROSCOPY INSTRUMENT	39
FIGURE 4-1 RESULTS FROM DETERMINATION OF THE FLOCCULATION POINT USING DICHLOROMETHANE AND PENTANE AS SOLVENTS. AT A VOLUME RATIO OF 1.5 PENTANE-TO-DICHLOROMETHANE THE ASPHALTENES START TO PRECIPITATE WHICH IS THE FLOCCULATION POINT	42
FIGURE 4-2 RELATIVE UV ABSORBANCE VS. CUMULATIVE VOLUME ELUTED FROM THE COLUMN FOR 12 FRACTIONS. MAXIMUM ABSORBANCE IS OBSERVED FOR FRACTIONS 2 AND 3 ACCORDING TO THE ELUTION VOLUMES IN TABLE 4-2.....	45
FIGURE 4-3 ASPHALTENE RECOVERY PERCENTAGE VS. VOLUME PERCENTAGE OF PENTANE IN SOLUTION.....	48
FIGURE 4-4 FLUORESCENCE OF FIVE DIFFERENT FRACTIONS ELUTED FROM THE COLUMN FOR THREE DIFFERENT SOLVENT MIXTURES USING SEA SAND AS CHROMATOGRAPHY PACKING. AN EXCITATION WAVELENGTH OF 440 NM WAS SELECTED FOR ALL THREE EXPERIMENTS	50
FIGURE 4-5 FLUORESCENCE SPECTRA OF FIVE FRACTIONS FROM SEA SAND, SAND ACID TREATED AND SAND BASE TREATED AT THE FLOCCULATION ONSET CONDITION. AN EXCITATION WAVELENGTH OF 440 NM WAS SELECTED FOR ALL THREE CASES.	52

FIGURE 4-6 CUMULATIVE ASPHALTENE AND METAL RECOVERY PERCENTAGE AT A SOLUBILITY PARAMETER OF 17.0 MPa^{0.5} FOR SOLVENT MIXTURE.....	56
FIGURE 4-7 CUMULATIVE ASPHALTENE AND METAL RECOVERY PERCENTAGE AT A SOLUBILITY PARAMETER OF 18.2 MPa^{0.5}	57
FIGURE 4-8 FLUORESCENCE SPECTRA OF 12 FRACTIONS ELUTED FROM THE COLUMN AT ROOM TEMPERATURE. AN EXCITATION WAVELENGTH OF 440 NM WAS SELECTED FOR TOLUENE/HEXANE MIXTURE AT ROOM TEMPERATURE.....	60
FIGURE 4-9 FLUORESCENCE SPECTRA OF 12 FRACTIONS ELUTED FROM THE COLUMN AT 50°C TEMPERATURE. AN EXCITATION WAVELENGTH OF 440 NM WAS SELECTED ANALYSIS OF SOLUTIONS IN HEXANE/TOLUENE AT ROOM TEMPERATURE.	61
FIGURE 5-1 METAL RECOVERY PERCENTAGE OF ALKALINE EARTH METAL MODIFIED SILICA MATERIALS USED AS A CHROMATOGRAPHY PACKING. A VOLUME RATION OF 0.55/0.45 OF PENTANE/DICHLOROMETHANE WAS USED AS A SOLVENT MIXTURE.	69
FIGURE 5-2 FTIR PLOTS FOR FIVE DIFFERENT SILICA MATERIALS USED AS CHROMATOGRAPHY PACKING. THE SPECTRA WERE SCALED TO GIVE THE SAME OFFSET BETWEEN THE PLOTS.....	71
FIGURE 5-3 PLOT OF RECOVERY OF ASPHALTENE AND VANADIUM VERSUS SURFACE CONCENTRATION OF ADDED CATION.	73
FIGURE 5-4 FLUORESCENCE SPECTRA OF 12 FRACTIONS FROM SILICA (UNTREATED)..	74
FIGURE 5-5 FLUORESCENCE SPECTRA OF 12 FRACTIONS FROM SILICA TREATED WITH MG.	75
FIGURE 5-6 FLUORESCENCE SPECTRA OF 12 FRACTIONS FROM SILICA TREATED WITH CA	76
FIGURE 5-7 FLUORESCENCE SPECTRA OF 12 FRACTIONS FROM SILICA TREATED WITH BA	77
FIGURE 5-8 FLUORESCENCE SPECTRA OF 12 FRACTIONS FROM SILICA TREATED WITH SR.	78
FIGURE 7-1 FTIR PLOTS FOR LUDOX TREATED WITH BA IONS.....	84
FIGURE 7-2 FTIR PLOTS FOR LUDOX TREATED WITH CA IONS	85
FIGURE 7-3 FTIR PLOTS FOR LUDOX TREATED WITH MG IONS	86
FIGURE 7-4 FTIR PLOTS FOR LUDOX TREATED WITH SR IONS	87

LIST OF TABLES

TABLE 2-1 METAL COMPOUNDS IN ALBERTA BITUMEN (STRONG AND FILBY, 1991).....	7
TABLE 2-2 ELEMENTAL COMPOSITION OF C7-ASPHALTENES CONSTRUCTED FROM DATA OF (SISKIN, KELEMEN ET AL. 2006)	8
TABLE 3-1 ELUTION VOLUMES FOR TWO DIFFERENT COLUMN SIZES	31
TABLE 3-2 ELUTION VOLUMES FOR TWO DIFFERENT MASSES OF CHROMATOGRAPHY PACKING.....	33
TABLE 3-3 SP SYSTEM OPERATIONAL PERFORMANCE SPECIFICATIONS.....	37
TABLE 4-1 COLOR TREND AND WEIGHT OF ASPHALTENE IN EACH FRACTION COLLECTED FROM OPEN COLUMN CHROMATOGRAPHY, USING A COLUMN WITH 50 MG OF SAMPLE AND 230 G OF PACKING.....	43
TABLE 4-2 ELUTION VOLUME AND ASPHALTENE RECOVERY RATIO FOR ONE SINGLE SEPARATION OF COLD LAKE ASPHALTENES ON SEA SAND BY FLASH CHROMATOGRAPHY. FLOW RATE = 9 mL/MIN, 59 MG OF SAMPLE ON 250G OF PACKING	44
TABLE 4-3 SOLUBILITY PARAMETER, MOLAR VOLUMES AND VOLUME FRACTION OF SOLVENT USED IN THE SOLVENT MIXTURE	47
TABLE 4-4 ASPHALTENE RECOVERY PERCENTAGE FOR THREE DIFFERENT SOLUBILITY PARAMETERS AND VOLUME RATIOS OF PENTANE-TO-DICHLOROMETHANE IN THE SOLVENT MIXTURE.....	47
TABLE 4-5 MAXIMUM PEAK INTENSITIES AND WAVELENGTHS FOR FRACTIONS 2-5	49
TABLE 4-6 RECOVERY OF ASPHALTENES FROM FOR SEA SAND WASHED WITH ACID AND BASE, USING A SOLVENT MIXTURE WITH A SOLUBILITY PARAMETER OF 17.0 MPa^{0.5} ...	51
TABLE 4-7 ATOMIC CONCENTRATIONS OF DIFFERENT COMPONENTS ON THE SURFACE OF SEA SAND ACCORDING TO XPS.....	53
TABLE 4-8 ASPHALTENE AND METAL RECOVERY PERCENTAGE FOR TWO DIFFERENT SOLUBILITY PARAMETERS OF SOLVENT MIXTURE (PENTANE AND DCM).....	55
TABLE 4-9 METAL AND ASPHALTENE RECOVERY PERCENTAGES FOR A SOLVENT MIXTURE OF TOLUENE / HEXANE AT TWO DIFFERENT TEMPERATURES.....	62
TABLE 5-1 HYDROTHERMAL TREATMENT CONDITIONS FOR MODIFICATION OF SILICA	67

TABLE 5-2 COLD LAKE ASPHALTENE RECOVERY PERCENTAGE FROM 5 DIFFERENT SILICA MATERIALS 68

TABLE 5-3 ATOMIC CONCENTRATION RATIOS ON SURFACE OF 5 DIFFERENT SILICA MATERIALS 72

TABLE 8-1 HYDROTHERMAL PREPARATIONS FOR MODIFICATION OF SILICA MATERIALS. 88

TABLE 8-2 CUMULATIVE ASPHALTENE AND METAL RECOVERIES FOR DIFFERENT SILICA MATERIALS 89

TABLE 9-1 Ni CONCENTRATIONS OBTAINED FROM ICP ANALYSIS. DIFFERENT CONCENTRATIONS ARE OBTAINED USING DIFFERENT SOLVENTS, CHROMATOGRAPHY PACKINGS AND COLUMN TEMPERATURES. 90

NOMENCLATURE

I = Intensity, A.U

v_p = Volume fraction of pentane

v_D = Volume fraction of dichloromethane

v_H = Volume fraction of hexane

v_T = Volume fraction of toluene

λ_{\max} = Maximum wavelength, nm

δ_p = Solubility parameter of pentane, MPa^{0.5}

δ_D = Solubility parameter of dichloromethane, MPa^{0.5}

R = Scaling ratio

Chapter 1

Introduction

1.1 Background

Vanadium and nickel are the most troublesome metal complexes present in oil sands bitumen, heavy oils, and in the vacuum residue fraction of conventional petroleum. Although these metals are only present in trace quantities, they have significant detrimental impact on crude oil processing units in refineries. During combustion, the presence of vanadium compounds in product coke leads to the formation of vanadium pentoxide. A significant portion of this vanadium pentoxide is volatile and carried out with flue gases posing an environmental concern. Another important issue is the deactivation of catalysts by these metals, particularly FCC catalysts. Therefore, it is imperative that new technologies be developed for the selective removal of these contaminants from heavy oils and bitumen residua. These metals occur mainly in the “asphaltene” fraction of the oil, the fraction that precipitates in an n-alkane solvent and which includes the highest molecular weight components of the bitumen. The only commercial methods for their removal are precipitation and catalytic hydro processing.

The vanadium and nickel compounds are mainly associated with the asphaltene fraction of bitumen, defined as the fraction of the bitumen that precipitates in n-alkane solvents such as n-pentane or n-heptane, and this method is the basis for laboratory separations.

The current technology for separation of the asphaltenic components from bitumen uses solvent precipitation, both in laboratory separations and on an industrial scale. In the Muskeg River mine froth treatment process at the highest solvent/bitumen ratio of 10, 60% of the vanadium and nickel is rejected along with approximately 90% of C₅ asphaltenes (Long 2006).

Even with removal of over 10% of the bitumen as C₅ asphaltenes, a significant portion of the metals still remain in bitumen. Extraction with solvent like acetone was also used in a laboratory scale to separate petroleum and different fractions with different polarities were obtained in this method. The disadvantage in this method is that the experiments should be performed at very low temperatures due to the high volatility of acetone. Also, large volumes of solvent should be prepared in order to achieve reproducibility of the experimental results (Speight 2006). Apart from the above techniques and solvent extraction of precipitated asphaltenes with acetone, no commercial or laboratory techniques are available for separation of organometallic compounds from crude oils. Conventional adsorbents such as γ -alumina or silica gel, adsorb asphaltenes so strongly that they can only be regenerated at high temperatures or by combustion. Laboratory separations of asphaltenes are not selective for the metal components. For example, these compounds occurred in all fractions that are separated using gel-permutation chromatography (Ignasiak et al. 1983). A number of studies have prepared porphyrin extracts for detailed characterization of structure by mass spectrometry, but these methods begin with precipitation and achieve very poor recovery of the total vanadium

and nickel from residue fractions. For example, the procedure of Nali et al. (1994) recovered only 10% of the metals for detailed characterization.

Several reaction methods are effective for metals removal. In industrial processing, thermal cracking combined with catalytic hydrogenation can remove most of the organometallic materials from bitumen. Unfortunately; the metals deposit in the catalyst as vanadium and nickel sulfides, giving irreversible deactivation (Munoz et al. 1994). This process also requires high pressure to achieve conversion. Alternative methods such as ultra filtration (Duong and Smith 1997) have been reported, but fouling was a persistent problem. Shiraishi et al. (2000) removed over 70% of the organometallic compounds from vacuum residue by photochemical treatment, combining photo irradiation with addition of 2-propanol as a hydrogen-bonding polar solvent. This approach gave low temperature removal, but the opacity of vacuum residue is a significant barrier to photochemical treatment.

Very little research has been conducted on selective adsorbents for removal of organometallic compounds, or sub fractions of the asphaltenes. Sakanishi et al. (1997) reported on the use of ion-exchange resins and activated carbon for asphaltene separation from diluted vacuum residue, but the recovery of metals on these solids was poor. Fractional precipitation by solvent mixtures also gave little or no selectivity for organometallic compounds (Sułkowskia 2005). As noted above, conventional metal-

oxide adsorbents interact too strongly with asphaltenes to be effective for removing organometallic components.

1.2 Research Approach

In this study, we investigated the use of silica materials to separate V and Ni compounds. We used high performance flash chromatography (HPFC) separation method to separate asphaltenes at different solvent strengths on sea sand. The separation conditions were optimized for flow rate and the strength of the solvent. The selectivity of the separation was evaluated based on three indicators: the recovery of the asphaltenes from the column, the recovery of the vanadium compounds, and the fluorescence spectra of the recovered material. The resulting separation method was then used to compare the performance of a series of silica materials treated with alkaline earth metals. These samples had a common silica support and were treated with the same molar concentration of reactant at the same temperature. The goal was to achieve high recovery of asphaltenes and high retention of the vanadium on the packings.

Chapter 2

Literature review

2.1 Chemistry of Vanadium and Nickel in Bitumen

Almost all crude oils and bitumen contain detectable amounts of vanadium and nickel porphyrins. Lighter crude oils only contain a small amount of these compounds. Heavy oils may contain large amounts of vanadyl and nickel porphyrins. A substantial amount of the vanadium in this crude oil is within the porphyrin structure. In high-sulfur crude oils which have a marine origin, there are more vanadyl porphyrins than nickel porphyrins. Low-sulfur crude oils which have other origins, usually contain more nickel porphyrins than vanadyl porphyrins. Of all the metals in the periodic table, only vanadium and nickel have been proven definitely to exist in significant amounts in a large number of crude oils and oil sand bitumen.

2.1.1 Chemistry of vanadium in bitumen

There are two types of nitrogen containing compounds in bitumen: the non-basic nitrogen-containing compounds and the basic nitrogen containing compounds. Porphyrins usually occur in the nonbasic portion of the nitrogen-containing concentrate. Porphine, which is the simplest porphyrin consists of four pyrrole molecules joined with one carbon linkage (Figure 2-1). These carbon linkages are methylene bridges and extend

the resonance system inside the porphine structure (Speight 2006). In crude oils and bitumens, the centre of the ring is occupied by a vanadyl group (V=O) or nickel.

A large number of different porphyrin compounds exist in nature or have been synthesized. Most of these compounds have substituents other than hydrogen on many of the ring carbons. For example, porphyrin rings substituted with four ethyl groups are commonly found in petroleum and bitumen.

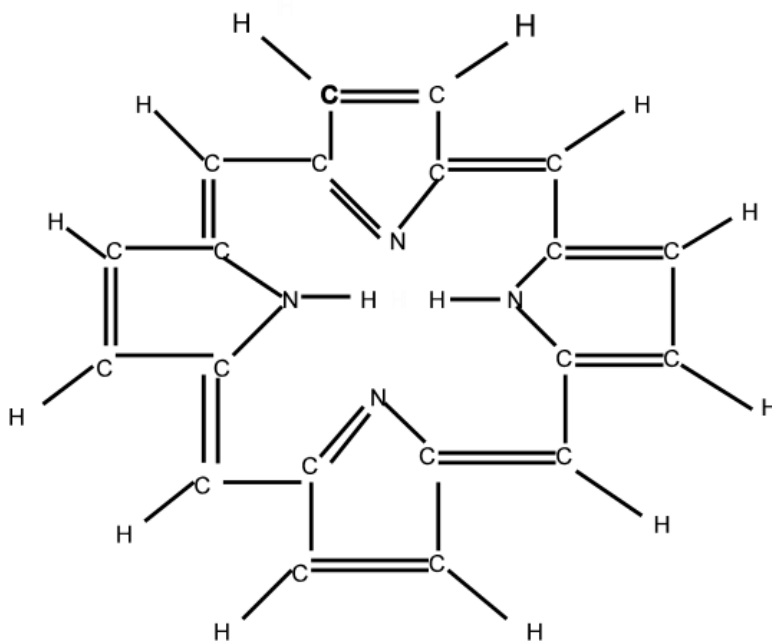


Figure 2-1 Porphine-the basic structure of porphyrins, (Speight 2006)

If the vanadium and nickel contents of crude oil are measured and compared with porphyrin concentrations, it is usually found that not all the metal content can be accounted for as porphyrins based on UV-visible extinction coefficients (Dunning et al.1960 and Fish et al. 1987) . In some crude oils, as little as 10% w/w of total metals appears to be within the porphyrin structures. Only rarely can all measured nickel and

vanadium in crude oil be accounted for as porphyrinic based on UV-visible spectrometry (Andreson 1988). While some investigators suggested that part of the vanadium and nickel in crude oils is chelated with ligands that are not porphyrins (Crouch et al. 1983 and Fish et al. 1984) the current consensus is that interactions of porphyrins with other components in the crude oil and substitutions on the porphyrin ring account for the lower than expected UV-visible absorption.

2.1.2 Concentrations of metals in bitumen materials

Strong and Filby (1987, 1991) have studied Alberta bitumen and have reported the vanadium, vanadium porphyrins and nickel concentrations in Alberta bitumen as well. (Table 2-1)

Table 2-1 Metal compounds in Alberta bitumen (Strong and Filby, 1991)

Property	Athabasca	Peace River	Cold Lake
V, ppm	196	180	191
Ni, ppm	75	62	63

2.2 Chemistry of Asphaltenes

Asphaltenes are defined as the material which is soluble in benzene (or toluene) and insoluble when diluted with large excess of n-alkane (pentane or heptanes). Asphaltenes

have high aromatic carbon content, consistent with the H/C ratio and low hydrogen content.

Table 2-2 Elemental composition of C7-asphaltenes constructed from data of (Siskin, Kelemen et al. 2006)

C7-asphaltene	Element Weight%					Metal, ppmw	
	C	H	S	N	O	Ni	V
Campana	87.6	8.2	0.5	1.5	2.2	54	81
Heavy Canadian	84.7	7.9	4.5	1.2	1.6	320	697
Lloydminster Wainwright	80.0	8.0	7.9	1.3	2.7	417	1100
Maya	82.3	7.9	6.6	1.2	1.8	724	1468
Mid-Continent U.S.	84.9	8.6	3.8	1.0	1.6	188	309
San Joaquin Valley	84.5	8.3	2.3	2.6	2.3	594	540

There have been considerable efforts by analytical chemists to characterize the asphaltenes in terms of chemical structure. Physical methods include IR, NMR, ESR, mass spectrometry, x-ray, ultracentrifugation, electron microscopy, VPO, GPC, etc. Chemical methods involve oxidation, hydrogenation, etc. One representative structure for resin and asphaltene molecules belong to the Athabasca crude (Suzuki et al. 1982) and includes carbon, hydrogen, oxygen, nitrogen, sulphur as well as polar and non-polar groups as shown by Figure 2-2. Asphaltenes differ from polycyclic aromatic hydrocarbons due to the presence of oxygen and sulfur in varied amounts.

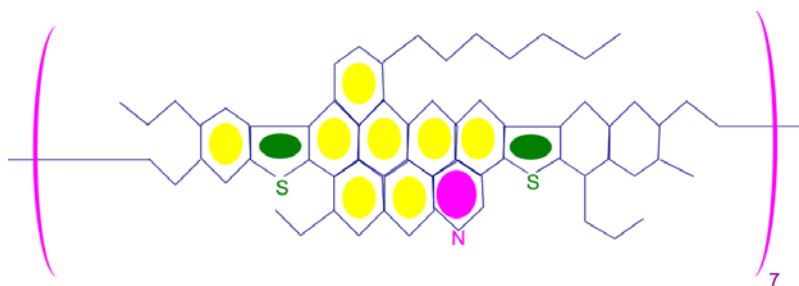


Figure 2-2 Average molecular structural models of asphaltene fraction of petroleum (Suzuki 1982)

2.3 Basis for asphaltene color

Different compounds have different colors due to electronic behavior of the materials in solution. For example, chlorophyll is green; the 2, 4-dinitrophenylhydrazone derivatives of aldehydes and ketones range in color from bright yellow to deep red, and water is colorless. The light reflected from the surface of a solid or passing through a liquid is analyzed by human eye, which acts as a spectrometer to detect different colors (Reusch 1999). As discussed in the previous section, asphaltene is a complex mixture which has a black color. If this complex mixture is separated into different fractions, different colors could be observed for the separated fractions, in theory, if the compounds within the fractions had the same absorption and fluorescence properties.

2.4 Spectroscopy of Asphaltenes

2.4.1 UV-Visible Spectroscopy

When sample molecules are exposed to light having an energy that matches a possible electronic transition within the molecule, some of the light energy will be absorbed as the electron is promoted to a higher energy orbital (Reusch 1999). The wavelengths at which adsorption occurs, and the degree of absorption at each wavelength are recorded with an optical spectrometer and a graph of absorbance (A) versus wavelength is presented. If a substance is colorless, it does not absorb the visible part of the spectrum and this region is not displayed on the graph. (Ingle and Crouch, 1988). The absorbance scale usually ranges from 0 (no absorption) to 2 (99% absorption). By UV-visible spectroscopy, concentrations of absorbing components are measured by using the Beer-Lambert law

$$A = -\log_{10}(I/I_0) = \epsilon \times c \times L \quad (2.1)$$

Where A is the measured absorbance, I_0 is the intensity of the incident light at a given wavelength, I is the transmitted intensity, L the path length through the sample, and c the concentration of the absorbing species. The molar absorptivity or extinction coefficient (ϵ) is a constant for each species and wavelength if the concentration is low enough to avoid intermolecular interactions in solution. This constant is a fundamental molecular property of a solute in a given solvent, at a particular temperature and pressure, and has units of $1 / M * cm$ or often $AU / M * cm$. If the molecule is very complex or bound to other species in solution, then the extinction coefficient changes. In complex petroleum mixtures, therefore, the extinction coefficient may depend on other components. (Evdokimov et al. 2003)

Fedorak et al. (1993) were able to determine the apparent petroporphyrin content of the various fractions of Cold Lake asphaltenes from the UV-visible spectrum at a wavelength of 410 nm, which is known as the Soret band. The absorbance at 410 nm was used for determination of porphyrin concentration with a known value of the extinction coefficient of the porphyrin.

2.4.2 Fluorescence spectroscopy of asphaltene solutions

Fluorescence spectroscopy is widely used to study asphaltene properties in solutions (e.g. toluene solutions). In fluorescence spectroscopy, the species is first excited, by absorbing a photon, from its ground electronic state to one of the various vibrational states in the excited electronic state. (Rendell, D. 1987). The wavelength of absorption is related to the size of the chromophores. Smaller chromophores correspond to higher energy (shorter wavelength). Interactions with other molecules in solution cause the excited molecules to emit a photon in the process. As molecules may drop down into any of several vibrational levels in the ground state, the emitted photons will have different energies, and thus frequencies. (Sharma and Schulman, 1999). Therefore, by analyzing the different frequencies of light emitted in fluorescent spectroscopy, along with their relative intensities, the structure of the different vibrational levels can be determined. (Lakowicz. 1999).

In a typical experiment, the different frequencies of fluorescent light emitted by a sample are measured, holding the excitation light at a constant wavelength which gives an

emission spectrum. These interactions cause the excited molecules to lose the energy and again reach the ground state of energy. Strausz et al. (2009) reexamined a theory which indicated that the fluorescence intensity of asphaltenes depends on the molecular weight of the asphaltene. By gel- permeation- chromatography, they were able to separate asphaltenes into different fractions with different molecular weights. They observed that as the chromophore size increases, the excitation energy decreases. This would lead to an increase in the rate of $S_0 \rightarrow S_1$ transition resulting in the suppression of fluorescence intensity with an increasing of molecular weight in separated asphaltene fractions.

Relatively few studies have been done on fluorescence spectroscopy of crude oils and asphaltenes and very little information is provided in this area in literature. Fluorescence emission spectra have been measured for ten different crude oils and different concentrations using a broad range of excitation wavelengths by (Downare and Mullins 1995). According to their studies, energy transfer results in significant shifts of peak intensity when shorter wavelength excitation is selected for heavier crude oils. Also, they concluded that all crude oils have the same emission spectra when long excitation wavelengths are selected. So the effects of energy transfer are not observed in the emission spectra in this case.

2.5 Aggregation of asphaltene components

According to studies by Takanohashi et al. (2003) , asphaltenes which are the heaviest and most polar compounds of oil, aggregate in solution to form complex colloidal structures. Aggregated asphaltenes precipitate from the oil upon dilution with solvents

such as pentane. They are known to form aggregated structure through various non-covalent interactions, such as aromatic-aromatic, electrostatic, and van der Waals interactions between the molecules because of their high aromaticity, polar functional groups, and molecular weight. Such aggregation obstructs oil-carrying pipelines by "fouling" or "flocculation," and causes operational problems at the refinery.

2.6 Solvent Fractionation of Asphaltenes

Castillo et al. (2001) studied asphaltene solubility in toluene solutions and were able to obtain three different fractions of asphaltenes with different solubility parameters by precipitating them with PNP (Para Nitro phenol). The solubility of each fraction at room temperature was determined by preparing saturated solutions. The solubility measurements in toluene solutions afforded the following results in g L^{-1} : A1, 0.00; A2, 1.14; and A3, 57 g L^{-1} . According to these studies, asphaltenes are a complex mixture with different solubility. Spiecker et al. (2003) studied the solubility behavior of asphaltene sub fractions asphaltenes from four different crude oils: Arab Heavy, B6, Canadon Seco, and Hondo were fractionated in mixtures of heptane and toluene solutions. After obtaining the solubility profiles of each fraction, they concluded that a particular subfraction with lower H/C ratio (higher aromaticity) has modestly higher V, N, Ni and Fe contents than the less polar and more soluble subfraction of the asphaltene.

(Yang 2004) studied six subfractions of Athabasca bitumen Asphaltenes by precipitatinion with increasing heptane/bitumen (H/B) ratio, from 1.25 to 40. Fourier

transform infrared (FTIR) spectroscopy, ultraviolet-visible(UV-vis) spectroscopy, and vapor pressure osmometry (VPO) were used in order to investigate the properties of Asphaltenes. They concluded that the first three asphaltene subfractions had lower H/C ratio or higher aromaticity and higher metalloporphyrin content . The last three subfractions had higher H/C ratios or less aromaticity and lower metalloporphyrin content.

2.7 Adsorption of Asphaltenes to surfaces

The effect of surface chemistry, asphaltene solubility and aggregation in solutions on asphaltene adsorption to surfaces will be discussed in the next sections. In the next section the reversibility of asphaltene adsorption is discussed according to findings in literature.

2.7.1 Reversibility of asphaltene adsorption

Reversibility of asphaltenes adsorption onto silica material was examined by several authors. For example, the very low desorption of asphaltenes (Figure 2-3) obtained by (Castillo et al. 2001) strongly suggests that adsorption is mainly an irreversible process. According to their studies, after adsorption of a monolayer on the surface, the asphaltenes bind to neighbor molecules on the surface, which results in building an insoluble network in toluene. Figure 2.3 shows the kinetic results for the desorption experiment. After 3000 min only 0.26% of the material initially adsorbed is desorbed in this experiment. These

slow changes are likely due to the build up of an insoluble network of asphaltenes on the solid surface.

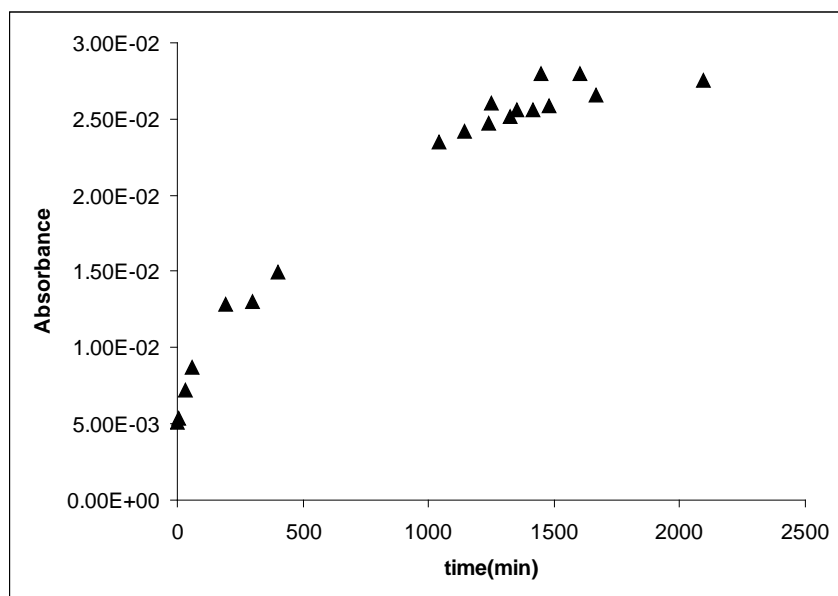


Figure 2-3 Desorption kinetics of Furrrial Asphaltenes from silica plate at room temperature in toluene. (Castillo, Fernández et al. 2001)

2.7.2 Effect of asphaltene aggregation and solubility on adsorption

As mentioned in the previous sections, asphaltenes have a high tendency to self associate and form aggregates in solution. Spiecker et al. (2003) indicated that the less soluble subfractions formed aggregates that were considerably larger than the more soluble subfractions. Off course, solubility and adsorption are related phenomena, and thus it could be expected that the less-soluble fraction that has a high tendency to self associate in solution, will be adsorbed first. Castillo et al. concluded that the fraction of asphaltenes

which has a high tendency to aggregate in toluene solutions also has a high tendency to adsorb on to the surface of silica material.

2.7.3 Effect of surface chemistry of the adsorbent

Another important factor which affects asphaltene adsorption on surfaces is the surface chemistry of the adsorbent. Different attempts have been made to explain the effect of surface chemistry of the adsorbent on asphaltene adsorption. These works are discussed in this section.

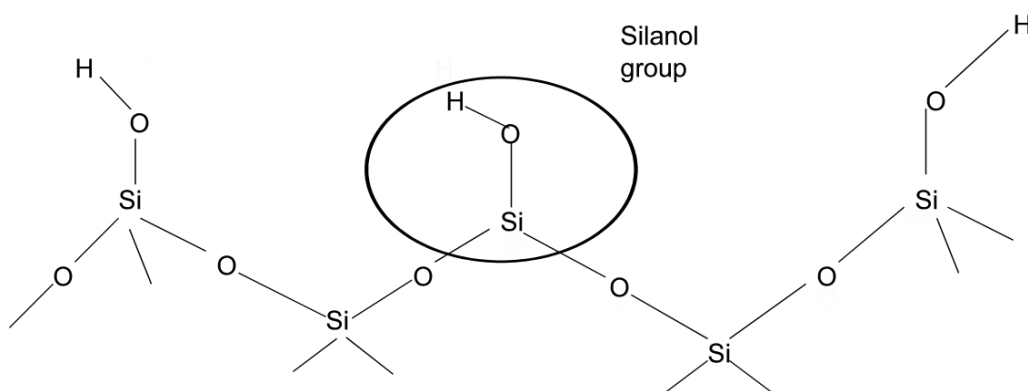


Figure 2-4 Silanol groups on surface of silica material

Since asphaltene is a mixture of different compounds, it is difficult to explain the effect of different surface chemistries on asphaltene adsorption. Silica materials, as mentioned in the next section, are known for possessing O-H groups on their surface. Ikoma et al. (2001) examined the adsorption behavior of different silica-metal oxide particles for different types of simple components. The mobile phase was 1% methanol/n-hexane and they used pyridine, benzene and dimethyl phthalate as test samples. Surface

characteristics were reported for silica-zirconia, silica-alumina, silica-titania, silica-magnesia, and silica gel. These include Si/metal ratio and acidity of solids measured by amine titration method with 4 indicators.

According to the results for solid acidity, silica-magnesia had weaker solid acidity than the other packings. Silica gel has the lowest acidity among all chromatography packings.

Chromatography was done on silica gel and mixed-oxide gels and the silica-magnesia gel showed the most appropriate separation behavior. With silica-zirconia benzene, dimethylphthalate eluted, but pyridine which is a basic compound, did not elute. With silica-magnesia and silica-titania the elution of benzene, dimethylphthalate and pyridine was observed from the chromatogram with silica gel, pyridine did not elute at all. Silica gel has been known to possess the large adsorption capacity for basic compounds. Based on the described work, silica magnesia had the best separation ability, particularly for a basic compound depending on the reduction of the activity of silanol groups on the silica surface. According to retention characteristics of mixed-oxide gel, the ability of mixed-oxide gels for basic compounds is considered as follows: Silica~ Silica-Zirconia » Silica-Alumina » Silica-titania » Silica-magnesia

Dudarev et al. (2008) studied the effect of different surface chemistry on asphaltene adsorption. They concluded that the lowest adsorption of all the examined solid surfaces were hydrophobic silica, which has less OH groups. Previously in literature, (Buckley and Liu 1998) concluded that polar interactions between polar groups of the crude oil and

hydroxyl groups on the surface happen in the absence of water and these groups are responsible for adsorption of asphaltenes on minerals and clay.

Yin et al. (2009) studied asphaltene adsorption on C₁₈-silica gel and they were able to remove over 50% of vanadium and nickel from different asphaltenic materials and they observed that the asphaltene adsorption on modified silica gel surfaces was minimal (less than 10%).

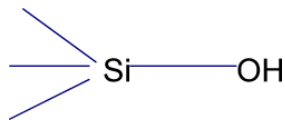
2.8 Silica Adsorbents

2.8.1 Surface chemistry

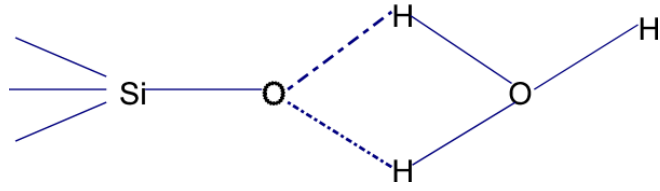
Silica adsorbents are oxygen-containing compounds which are typically hydrophilic and polar. Therefore, silica is used for drying of process air (e.g. oxygen, natural gas) and adsorption of heavy (polar) hydrocarbons from natural gas.

2.8.1.1 Types of surface hydroxyl-groups

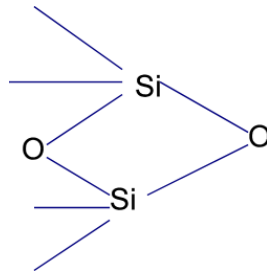
There are five different types of adsorption sites on the surface of the fully hydroxylated silica: (Board 2003)



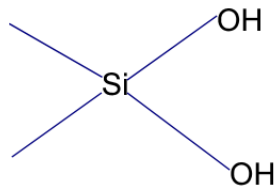
1. Free silanol



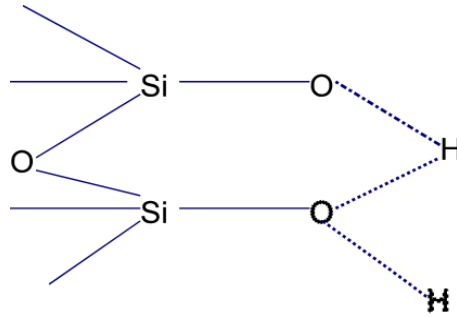
2. Silanol groups with physically adsorbed water



3. Siloxane bonds



4. Geminal silanol groups



5. Hydrogen-bonded silanol groups

Figure 2-5 Different silanol groups

The maximum concentration of silanol groups on the surface of porous silica is 8 to 9 $\mu\text{mol}/\text{m}^2$ or around 5 -OH groups per 100×10^{-10} meters. (Baxter et al. 1997) These silanol groups correspond to the surface activity of silica materials. Because of the high concentration of silanol groups on the surface of silica gel, these materials have a high surface energy density.

2.9 Basic principles of chromatography

Chromatography is the most important separation method for all areas of science, even very complex mixtures, because it is a simple and practical method. Two types of chromatography are used: liquid phase chromatography and gas phase chromatography. The separated fractions are immediately available for both qualitative and quantitative analysis. The outcome of a chromatography experiment is a chromatogram.

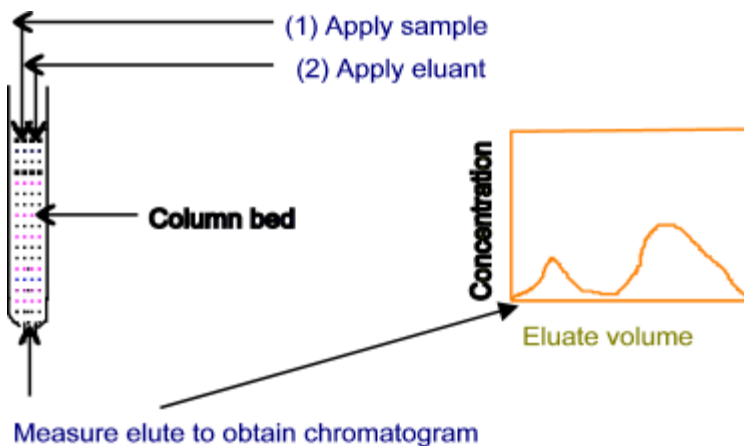


Figure 2-6 Schematic of column chromatography setup.

All chromatographic systems contain a stationary phase, a mobile phase and sample molecules (the mixture for separation). The basis for chromatography separations is the difference in retention time achieved for different compounds when the mixture is injected into the column. Chemical interactions between different compounds and the surface of chromatography packing and also the difference in the size of the molecules injected in to the column cause different retention times.

High performance flash chromatography (HPLC) methods have been developed to replace labor-intensive open-column liquid chromatography. Its applications include hydrocarbon-type separation, quantitative and qualitative analysis of petroleum. In this case, the solvent is driven through the column by applying positive pressure with a pump. (Snyder 2006). This allows less solvent usage and less time for separation which is beneficial for all type of (HPLC) applications. The modern flash chromatography systems are sold with pre-packed columns, but in this study, we designed the preparation

conditions for the packings used for our separations with flash chromatography system.(McPolin 2007).

2.10 References

1. Andreson, J. L. (1988). Advances In Chemical Engineering, Academic Press Inc.
2. Board, N. (2003). Modern Technology of Surface Coating with Formulae & Their Applications, Asia Pacific Business Press Inc.
3. Buckley, J. S. and Y. Liu (1998). "Some mechanisms of crude oil/brine/solid interactions." Journal of Petroleum Science and Engineering **20**(3-4): 155-160.
4. Castillo, J., A. Fernández, et al. (2001). "New techniques and methods for the study of aggregation, adsorption, and solubility of asphaltenes. Impact of these properties on colloidal structure and flocculation." Petroleum Science and Technology **19**(1-2): 75-106.
5. Crouch, F. W., C. S. Sommer, et al. (1983). "FRACTIONATIONS OF NONPORPHYRIN COMPLEXES OF VANADIUM AND NICKEL FROM BOSCAN CRUDE OIL." Separation Science and Technology **18**(7): 603-634.
6. Downare, T. D. and O. C. Mullins (1995). "Visible and near-infrared fluorescence of crude oils." Applied Spectroscopy **49**(6): 754-764.
7. Dudarova, D., S. Simon, et al. (2008). "Study of asphaltenes adsorption onto different minerals and clays. Part 1. Experimental adsorption with UV depletion detection." Colloids and Surfaces A: Physicochemical and Engineering Aspects **317**(1-3): 1-9.
8. Dunning, H. N., J. W. Moore, et al. (1960). "Porphyrin, nickel, vanadium, and nitrogen in petroleum." Journal of Chemical and Engineering Data **5**(4): 546-549.

9. Duong, A. and K. J. Smith (1997). "A Model of Ceramic Membrane Fouling during Heavy Oil Ultrafiltration." Canadian Journal of Chemical Engineering **75**(6): 1122-1129.
10. Evdokimov, I. N., N. Y. Eliseev, et al. (2003). "Assembly of asphaltene molecular aggregates as studied by near-UV/visible spectroscopy II. Concentration dependencies of absorptivities." Journal of Petroleum Science and Engineering **37**(3-4): 145-152.
11. Fedorak, P. M., K. M. Semple, et al. (1993). "Chloroperoxidase-mediated modifications of petroporphyrins and asphaltenes." Enzyme and Microbial Technology **15**(5): 429-437.
12. Filby, R. H. and D. Strong (1991). Nickel (II) and vanadium (IV) complexes in Alberta oil-sand bitumens. AICHE Symposium Series.
13. Fish, R. H., J. J. Komlenic, et al. (1984). "Characterization and comparison of vanadyl and nickel compounds in heavy crude petroleums and asphaltenes by reverse-phase and size-exclusion liquid chromatography/graphite furnace atomic absorption spectrometry." Analytical Chemistry **56**(13): 2452-2460.
14. Fish, R. H., J. G. Reynolds, et al. (1987). MOLECULAR CHARACTERIZATION OF NICKEL AND VANADIUM NONPORPHYRIN COMPOUNDS FOUND IN HEAVY CRUDE PETROLEUMS AND BITUMENS. ACS Symposium Series.
15. Ignasiak, T. M., L. Kotlyar, et al. (1983). "Preparative gel permeation chromatography of Athabasca asphaltene and the relative polymer-forming propensity of the fractions." Fuel **62**(3): 363-369.
16. Ikoma, S., K. Nobuhara, et al. (2001). Surface properties of silica-titania and silica-zirconia mixed oxide gels. Studies in Surface Science and Catalysis. **132**: 765-768.

17. Long, W. J. P. a. Y. (2006). The Athabasca Oilsands Project: The Commercial Applications Of Innovations In Technology. Oilsands Conference. Edmonton, Alberta.
18. McPolin, O. (2007). "Brief Guide to HPLC Instruments."
19. Munoz, V. A., S. V. Ghorpadkar, et al. (1994). "Characterization of coke on spent hydroprocessing catalysts by optical microscopy." Energy & Fuels **8**(2): 426-434.
20. Nali, M., F. Corana, et al. (1994). "Separation and characterization of vanadium and nickel organometallic compounds in heavy crudes." Fuel Science and Technology International **12**(4): 593-611.
21. Office of water program operations(EPA), N. T. a. O. T. C. (1979). Analytical methods for trace metals. Cincinnati, EPA Instructional Resources Centre.
22. Reusch, W. (1999). An exceptional introduction to modern nmr spectroscopy.
23. Sakanishi, K., N. Yamashita, et al. (1997). "Depolymerization and demetallation treatments of asphaltene in vacuum residue." ACS Division of Petroleum Chemistry, Inc. Preprints **42**(2): 373-377.
24. Shiraishi, Y., T. Hirai, et al. (2000). "A novel demetalation process for vanadyl- and nickelporphyrins from petroleum residue by photochemical reaction and liquid-liquid extraction." Industrial and Engineering Chemistry Research **39**(5): 1345-1355.
25. Siskin, M., S. R. Kelemen, et al. (2006). "Asphaltene molecular structure and chemical influences on the morphology of coke produced in delayed coking." Energy and Fuels **20**(3): 1227-1234.

26. Speight, J. G. (2006). The chemistry and technology of petroleum, Chemical Industries.
27. Spiecker, P. M., K. L. Gawrys, et al. (2003). "Aggregation and solubility behavior of asphaltenes and their subfractions." Journal of Colloid and Interface Science **267**(1): 178-193.
28. Strausz, O. P., I. Safarik, et al. (2009). "Cause of asphaltene fluorescence intensity variation with molecular weight and its ramifications for laser ionization mass spectrometry." Energy and Fuels **23**(3): 1555-1562.
29. Strong, D. and R. H. Filby (1987). VANADYL PORPHYRIN DISTRIBUTION IN THE ALBERTA OIL-SAND BITUMENS. ACS Symposium Series.
30. Suzuki, T., Ito, Y., Takegami, Y. and Watanabe, Y. (1982). "Chemical Structure of Tar-Sand Bitumens by ¹³C and ¹H NMR Spectroscopy Method." Fuel **61**: pages 402-410.
31. Suzuki, T., M. Itoh, et al. (1982). "Chemical structure of tar-sand bitumens by ¹³C and ¹H n.m.r. spectroscopic methods." Fuel **61**(5): 402-410.
32. Takanohashi, T., S. Sato, et al. (2003). "Molecular dynamics simulation of structural relaxation of asphaltene aggregates." Petroleum Science and Technology **21**(3-4): 491-505.
33. Wiesław W. Sułkowskia, A. W., Barbara Szoltyś, Wioletta M. Bajdurb and Anna Sułkowskac (2005). "Preparation and properties of flocculants derived from polystyrene waste" Polymer Degradation and Stability **Volume 90** (Issue 2): Pages 272-280.

34. Xiaoli Yang, H. H., and Jan Czarnecki (2004). "Investigation of Subfractions of Athabasca Asphaltenes and Their Role in Emulsion Stability." Energy Fuels **18** 770–777.
35. Yin, C. X., J. M. Stryker, et al. (2009). "Separation of petroporphyrins from asphaltenes by chemical modification and selective affinity chromatography." Energy and Fuels **23**(5): 2600-2605.
36. Lakowicz, J. R. (1999). "Principles of Fluorescence Spectroscopy". Kluwer Academic / Plenum Publishers
37. Sharma, A. and Schulman, S. G. (1999). "Introduction to Fluorescence Spectroscopy". Wiley interscience
38. Rendell, D. (1987). "Fluorescence and Phosphorescence". Crown 8.
39. J. D. J. Ingle and S. R. Crouch (1988), "Spectrochemical Analysis", Prentice Hall, New Jersey
40. Lloyd R. Snyder and John W. Dolan (2006). High-Performance Gradient Elution
Wiley Interscience
41. Sperling, Michael B.; Welz, Bernhard (1999). "Atomic Absorption Spectrometry".
42. L'vov, B. V. (2005), "Fifty years of atomic absorption spectrometry", Analytical Chemistry 60: 382
43. Ian Baxter Lisa D. Cother, Carole Dupuy et al. (1997), "Hydrogen bonding to silanols" electronic conference on organometallic chemistry,

Chapter 3

Materials and methods

3.1 Materials

Washed Sea Sand (CAS 14808), purchased from Fisher Scientific (Mississauga, ON), was used as a chromatography packing for separations.

Different silica materials prepared from Ludox HS-40 (colloidal silica, 40wt% suspension in water, Sigma-Aldrich, Steinheim, Germany) were used as another type of chromatography packing. Hydrothermal preparation of different silica materials will be discussed in chapter 5.

Cold Lake asphaltene prepared by Imperial Oil with a vanadium content of 850 parts per million (ppm) and nickel content of 300 ppm (after ICP-MS analysis) was used for chromatography separations.

Dichloromethane (CAS 75092), Pentane (CAS 109660), Nitric acid (CAS 7697372), toluene (CAS 108-88-3) and hexane (CAS 110-54-3) were supplied by Fisher Scientific (Mississauga, ON).

3.2 Experimental Procedure

A titration test was carried out in order to find the solvent ration which the Asphaltenes start to precipitate. Approximately 0.05 g of asphaltene was weighed and a total volume of 100ml of solvent was used for this test. Two burettes were used to add dichloromethane and pentane into a jar which contained asphaltene in each run. At the beginning 100ml of dichloromethane and 0 ml of pentane was added to 0.05 g of asphaltene. Filtered paper (55 mm hole), was used and during filtration the solution was washed with pentane. The solids retained on the wall of the separation unit. The filter paper, an alumina cup and the solids on the filter paper were weighted. The alumina cup and filter paper were also weighted separately. The weight difference was the weight of the precipitated asphaltene. Different volumes of pentane and dichloromethane were added in each run and a plot of asphaltene precipitate vs. solvent ratio of pentane-to-dichloromethane was plotted. The ratio at which the asphaltene started to precipitate was determined as the flocculation point.

3.2.1 Chromatography packing preparation

Sea sand was acid and base washed for another set of chromatography separations. 10 mL of HCl was added to 1 liter of reverse osmosis (RO) water, and 300 mL of sea sand was added to the solution. The mixture was rinsed with 80 mL of RO water four times for a 1 hour period. Enough time is needed for sea sand to settle. Then sand was left to dry then put in an oven at about 70C for several hours (between 4 -8 hours), until the sand looked dry. For the case of base treatment, 4 g of NaOH was added to 1 liter of RO water and the rest of the steps were the same.

3.2.2 Chromatography experimental procedure

3.2.2.1 Open column chromatography

Experiments were performed with a Chem Glass CG-1162-36 large column with approximately 230 g of sea sand. Approximately 10 g of solvent mixture with a volume

ratio of $\frac{V_P}{V_D} = 1.2$ was used to dissolve circa 0.05 g of asphaltene. The solvent mixture

was added continuously to the column while collecting 10 g of each fraction from the bottom. The total time for running this experiment was approximately 50 min. Each fraction had a different color which corresponded to the fluorescent excitation by the room light and the absorbance.

3.2.2.2 Flash chromatography using sea sand as chromatography packing

The following ratio was held constant while transferring the separations to the flash chromatography system.

$$\text{Ratio} = \frac{\text{mass of asphaltene(g)}}{\text{mass of sea sand}} = \frac{0.0063}{27} = 2.3E - 4 \quad (3.1)$$

A small column size was used with approximately 28 g of sea sand. Circa 6 mg of asphaltene was dissolved in approximately 20ml solvent mixture. 140 mL of solvent mixture was pumped through the column with a flow rate of 20 mL/min to prime the column. A solvent composition of 45% volume percent of dichloromethane, balance pentane, and flow rate of 1 mL/min was selected. A maximum fraction volume of 3 mL was collected from the system for each fraction. A plot of intensity vs. fraction number or time (min) was given by the UV detector at a wavelength of 245 nm.

3.2.2.3 Scale up calculations for sea sand

The purpose for scale up was to achieve higher mass of material eluted from the column in order to quantify the vanadium content in fractions eluted from the column using inductive coupled plasma spectroscopy. With a constant mass ratio while transferring from a small column to a large column, with 250 g of sea sand used for a large column, we obtain 0.059 g of asphaltene.

$$R = \frac{V_{sea\ sand, large\ column}}{V_{sea\ sand, small\ column}} = \frac{M_{sea\ sand, large\ column}}{M_{sea\ sand, small\ column}} = \frac{250}{27} = 9 \quad (3.2)$$

Table 3-1 Elution volumes for two different column sizes

Column size	V _{maximum elution volume} (ml)	V _{total elution volume} (ml)
Small Column	3	60
Large Column	3×9=27	27×20= 540

Therefore, a glass column with a diameter of 25 mm and length of 470 mm (Chem Glass Company) was packed with 250 g of sea sand. 140 mL solvent mixture of $\frac{V_P}{V_D}$ was pumped through the column with a flow rate of 20 mL/min and to prime the column. Due to high volatility of the solvent mixture, Very low and inconsistent volumes were collected from the column. Solvent filters A and C were then introduced into the solvent reservoirs of pentane and dichloromethane in order to maximize the surface area and overcome the pressure drop in the system. A fixed ratio of 45% (this condition was

selected based on the flocculation point of the asphaltenes) and flow rate of 9 mL/min was selected. This flow rate was selected in order to keep the separation time the same as in the previous open column chromatography work. A maximum fraction volume of 27 mL per tube was collected. A plot of intensity vs. fraction number or time (min) was given by the UV detector in the system at a wavelength of 245 nm. The fluorescence spectroscopy emission spectra and UV plots were collected for each sample.

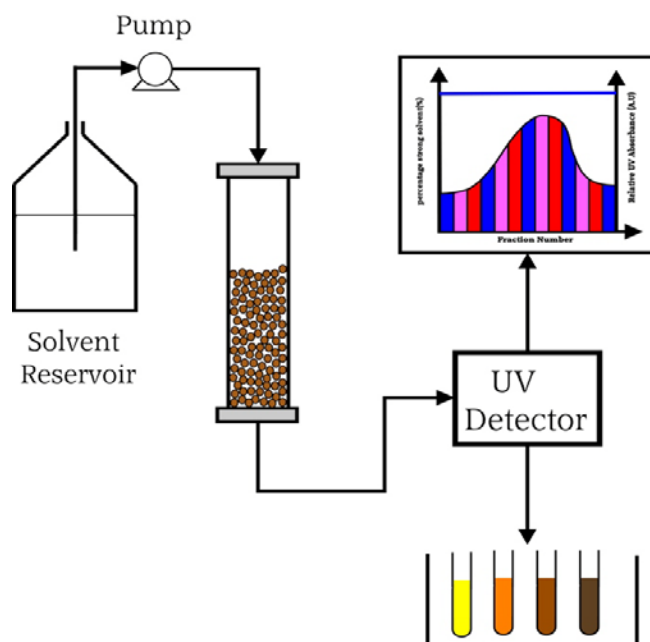


Figure 3-1 High Performance Flash Chromatography Assembly

3.2.2.4 Flash chromatography using modified silica materials as chromatography packing

The density of the modified silica samples was lower than the sea sand. The maximum mass of the silica material which would fill the large glass column was about 195.4 g.

$$R = \frac{\text{mass of asphaltene}(g)}{\text{mass of packing}(g)} = \frac{\chi}{195.4} = 2.3E - 4 \quad (3.3)$$

From the above equation, a value of $\chi = 0.046 \text{ g}$ is obtained for the total mass of asphaltene sample.

$$R_{\text{scale-up}} = \frac{V_{\text{Sea Sand}}(cc)}{V_{\text{Ludox}}(cc)} = \frac{310}{225} = 1.4 \quad (3.4)$$

Table 3-2 Elution volumes for two different masses of chromatography packing

Chromatography packing (large column)	V _{maximum elution volume} (ml)	V _{total elution volume} (ml)
Sea sand	27	540
Modified silica	27×1.4= 38	39×20= 780

Since the value of 38 ml was not activated in the instrument, the value of 39 ml for maximum elution volume was selected.

3.2.3 Experiments in hexane/toluene solution

3.2.3.1 Experiments performed at 50C

Heating tape was wrapped around the column and a thermocouple was inserted between the heating tape and the column (on the outside). The thermocouple indicated the temperature of the column during the whole experiment. The same amount of asphaltene described in section 3.2.2 was dissolved in a solvent mixture with a volume ratio of:0.4/0.6 hexane-to-toluene

The rest of the experimental procedures were the same as pentane/dichloromethane solvent mixtures.

3.2.3.2 Experiments performed at room temperature

The same amount of asphaltene was dissolved in the same solvent mixture described in section 3.2.3.1. The rest of the experimental procedure was the same as section 3.2.2.

3.2.4 Solvent evaporation

Solvent was evaporated from the fractions by allowing the samples to stand in a fume hood for several days. The total mass of material eluted from the column after separation was obtained by adding the weight of all collected fractions. In some experiments, all collected fractions were combined in a 500 ml volumetric flask, and most of the solvent was evaporated using a rotary evaporator and then was transferred to a smaller flask for final evaporation. . Since the solvent mixture is a volatile mixture, the temperature of the rotary evaporator was set at (50 °C) and vacuum was applied to evaporate the solvent in a 50 ml volumetric flask.

3.2.5 Acid digestion

Acid digestion was performed to prepare the samples for inductive coupled plasma (ICP) analysis. Nitric acid (5-10 mL) was added to each vial to dissolve the samples. The samples were heated to 200°C in a silicone oil bath with a Supernova hotplate (Fisher Scientific). The acid vapors were condensed with a condenser to avoid drying of samples. The duration of digestion was 2-3 days.

Checking the samples was necessary in order to make sure no solid deposits were obtained at the bottom of the flask. If solid deposits were observed, more time was given to digest the samples until no solid deposits were observed. The solution was transferred to a 50 ml volumetric flask and distilled water until a 50 ml solution was obtained. The flask was shaken carefully and finally the whole solution was transferred in to a 20 mL vial.

3.3 High Performance Flash Chromatography (HPFC)

The apparatus was a model SP1 HPFC system instructed by Biotage Company, US, with detailed specifications provided in Table 3-3 and analysis process illustrated in Figure 3-2.



Figure 3-2 SP1—the single-column flash purification system, image from Biotage company with permission.

Table 3-3 SP System Operational Performance Specifications

Total fraction volume	Maximum 2.9 L (standard)
Solvent inlets	4 inlets
Maximum Total Volume	2880 mL with no rack change (5760 mL with EXP systems)
Solvent delivery	Constant volume (3 mL) electric HPFC pump
Flow Rate	1 to 100 ml/min variable, in 1 mL/min increments
Solvent Delivery	Constant volume 3 mL/stroke electric HPFC pump
Pressure Resistance	100 psig maximum operating
UV Detector	Available in two models: Standard model with variable wavelength (200-320 nm) Optional model with fixed wavelength (254 nm)
Collection Vessels	Test tubes (mm): 13, 16, 17, 18, and 25, bottles (mL): 120 and 240

3.4 Analytical Methods

3.4.1 FT-IR spectroscopy

An IR spectrum represents a fingerprint of a sample with absorption peaks which correspond to the frequencies of vibrations between the bonds of the atoms making up the material. Because each different material is a unique combination of atoms, no two compounds produce the same IR spectrum. Therefore, IR spectroscopy can result in a positive identification (qualitative analysis) of every different kind of material. A beam of infrared light is produced and passed through the sample. Wavelengths between 700 cm^{-1} 4000 cm^{-1} were used and the transmittance of the IR beam for each sample was recorded. This analysis was done with a Nicolet 6700 FTIR spectrometer, manufactured by Thermo Fisher Scientific in USA.

3.4.2 X-ray Photoelectron Spectroscopy (XPS)

The XPS measurements were performed on AXIS 165 spectrometer (Kratos Analytical) at the Alberta Centre for Surface Engineering and Science (ACSES), University of Alberta to measure the atomic concentrations of Si, O and metal on the surface of silica material. The base pressure in the analytical chamber was lower than 2×10^{-8} Pa. The measurements are based on the photoelectric effect. In this process a photon with a well defined energy $h\nu$, hits the sample and is absorbed. If the photon energy is high enough, the excited electron escapes from the surface and their kinetic energy is roughly given by

$$\text{KE} = h\nu - \text{BE} - \phi \quad (3.1)$$

3.4.3 Fluorescence Spectroscopy

All experiments were performed at room temperature. Emission spectra were collected between 450 and 900 nm with a Cary Eclipse Spectrofluorimeter (Varian Inc., Australia) depending on the excitation wavelength. The maximum excitation intensity was obtained at 440 nm when the emission spectra were collected between 190 nm and 900 nm. Values of 0 and 1000 were chosen for the minimum and maximum intensity for the emission spectra.

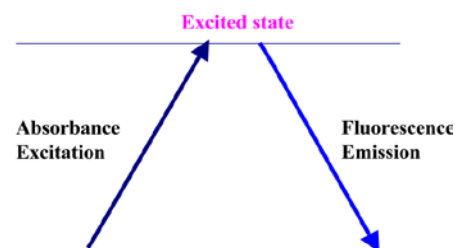
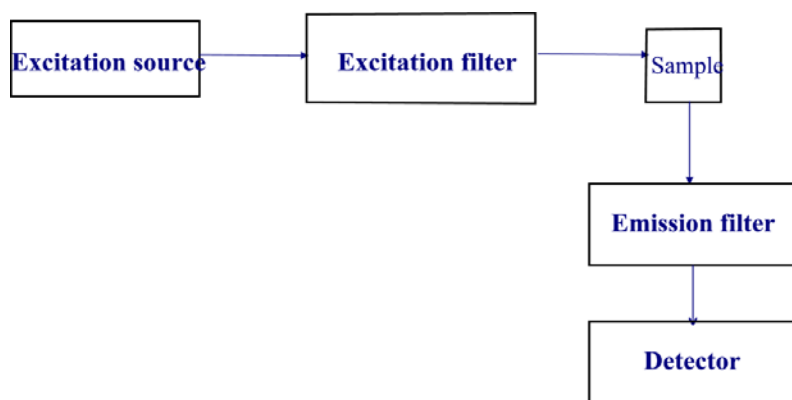


Figure 3-3 Fluorescence spectroscopy instrument



A single excitation wavelength of 440 nm was selected for each sample and the fluorescence spectrometer probe was introduced in each sample in order to observe emission spectra. Dilution with Dichloromethane was applied for fractions which would demonstrate a flat intensity peak or exceed an intensity value of 1000 A.U.

3.4.4 Inductive Coupled Plasma Spectroscopy

An ICP works by injecting a nebulized mist from a liquid into the centre of argon plasma. Plasma is created from a flow of gas within a high energy field (in the case of an ICP, by a strong alternating current of RF energy flowing in a coil just outside of the gas flow) which ionizes the gas and causes intense heating. Temperatures inside ICP plasma reach 10000 K- as hot as the surface of sun. When the mist of the sample enters the plasma, the intense heat causes the dissociation of most chemical compounds, and the energy that the component atoms adsorb causes them to undergo excitation and ionization energy transitions. These transitions produced by the plasma are broken down into individual lines into concentrations for a specified suite of elements.

ICP spectroscopic analysis was performed on acid-digested aqueous samples using a Perkin Elmer Elan 6000 (Department of Earth and Atmospheric Sciences, University of Alberta). The vanadium concentration was reported in ppm units for each vial. Four points were used for calibration curves (0, 0.005, 0.010, 0.020 ppm). The linear range was up to 10 ppm, but we can dilute samples to analyze them, so almost any concentration is detectable. The final results are the average of 3 replicates and reported in ppm on a sample weight basis.

Chapter 4

Results & Discussion of Separations on Sea Sand

4.1 Selection of solvent composition for chromatography of asphaltenes

The hypothesis for this study was that controlled surface chemistry on silica materials would enable selective removal of metal bearing components from asphaltenes and bitumens. Sea sand was selected as an initial test material, representing a silica surface with limited modification. Preliminary separations of Cold Lake asphaltenes on an open column of sea sand showed that use of strong solvents, such as toluene or dichloromethane, showed no evidence for selective separation based on color of eluted material. When weaker solvent mixtures were used, to reduce the competition between solvent and asphaltenes for adsorption sites on the packing, then colored fractions were observed to elute, indicating the emergence of a selective separation. In order to maximize the interaction of the asphaltenes with the packing, we decided to operate at a solvent composition near the flocculation point of the asphaltenes.

4.2 Determination of the flocculation point of asphaltenes for chromatographic separation

The results from determination of the flocculation point are shown in Figure 4-1. The flocculation point refers to the volume ratio of 0.55/0.45 (on a volume basis) pentane-to-

dichloromethane in the solvent mixture in which the asphaltenes start to precipitate. Scaling of separations between open column chromatography and flash chromatography was investigated using this volume ratio in the solvent mixture.

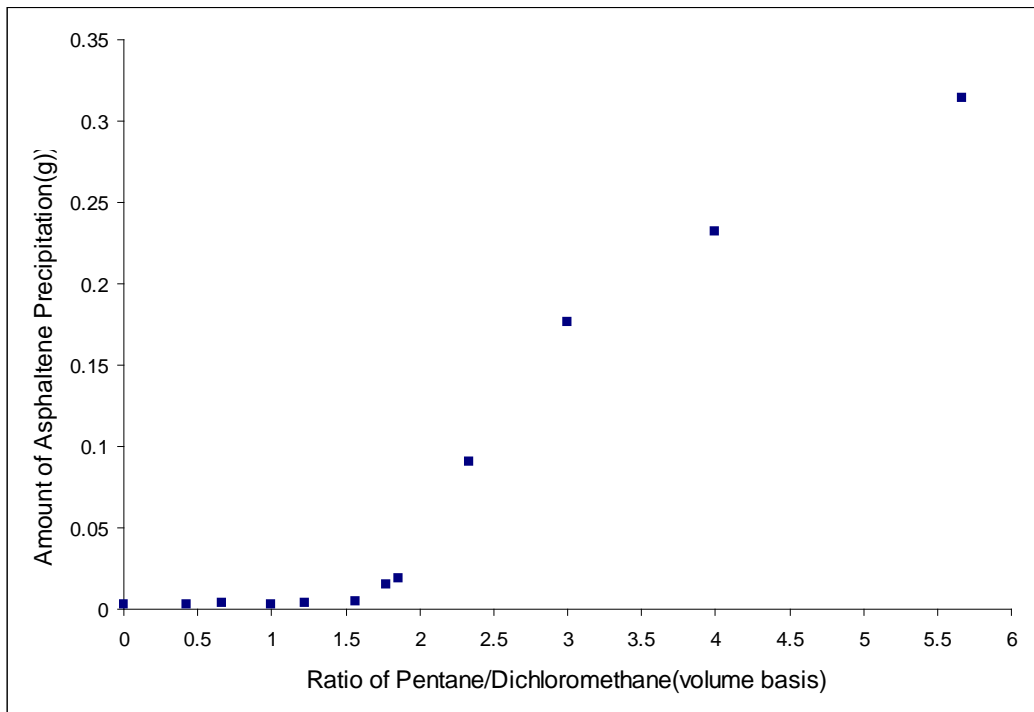


Figure 4-1 results from determination of the flocculation point using dichloromethane and pentane as solvents. At a volume ratio of 1.5 pentane-to-dichloromethane the asphaltenes start to precipitate which is the flocculation point

4.3 Recovery of Cold Lake asphaltenes from sea sand

The initial experiments used an open column with manual addition of solvent. The asphaltene recovery percentage was calculated using the following equation:

$$\text{Asphaltene recovery ratio} = \frac{\text{Total mass of material eluted from the column (mg)}}{\text{Mass of asphaltene used originally (mg)}} \quad (4.1)$$

The color trend of 10 fractions and the recovery percentage of the material eluted from the column using open column chromatography are presented in Table 4-1.

Table 4-1 Color trend and weight of asphaltene in each fraction collected from open column chromatography, using a column with 50 mg of sample and 230 g of packing

Fraction number	Color trend	Weight of asphaltene (mg)
1	Colorless	0.2
2	Colorless	0.5
3	Colorless	0.7
4	Colorless	0.9
5	Very yellow	3.2
6	Orange	4.2
7	Orange	1.7
8	Light orange	1.1
9	Yellow	0.8
10	Yellow	0.7

$$\text{Recovery}_{\text{open column}} = \frac{0.014}{0.0501} = 28\% \quad (4.2)$$

From the information provided in Table 4-1, different colors are observed for fractions 1-10 which is an indication of selectivity of separation. The mass of material eluted in each fraction and the recovery percentage both are indications of high retention of asphaltenes on the surface of sea sand. In order to improve the repeatability of the chromatographic

separations, the separations were repeated using a flash chromatography system. The recovery percentage of the material eluted from the column and the color trend of 12 fractions by flash chromatography is presented in Table 4-2.

Table 4-2 Elution volume and asphaltene recovery ratio for one single separation of Cold Lake asphaltenes on sea sand by flash chromatography. Flow rate = 9 mL/min, 59 mg of sample on 250g of packing

Elution volume(ml)	Color trend	Asphaltene weight (mg)
27	Colorless	0.3
54	Brown	10.5
81	Gold	4.5
108	Gold	1.4
135	Light yellow	0.2
162	Light yellow	0.2
189	Pale yellow	0.1
216	Pale yellow	0.1
243	Almost colorless	0.1
270	Colorless	0.1
297	Colorless	0.1
324	Colorless	0.1
Recovery Ratio	$\frac{0.01776}{0.05875} = 0.302$	

Comparison of Table 4-1 and Table 4-2 shows that the two separations gave a similar pattern of observed colors in the eluent, and similar overall recovery. The observation of different colors, by visual observation, indicated selective separation of some components

by this chromatographic method. The similar recovery using open column and flash chromatography methods shows that the scaling of the conditions between the two methods was successful. Consequently, the flash chromatography system was used as a replacement for the labor intensive method of open column chromatography. A plot of UV intensity vs. cumulative elution volume, are shown in Figure 4-2. The intensities correspond roughly to the mass of material eluted from the column. With fractions 2 and 3, the maximum intensity corresponds to the maximum mass eluted from the column which can be observed in Table 4-2 as well.

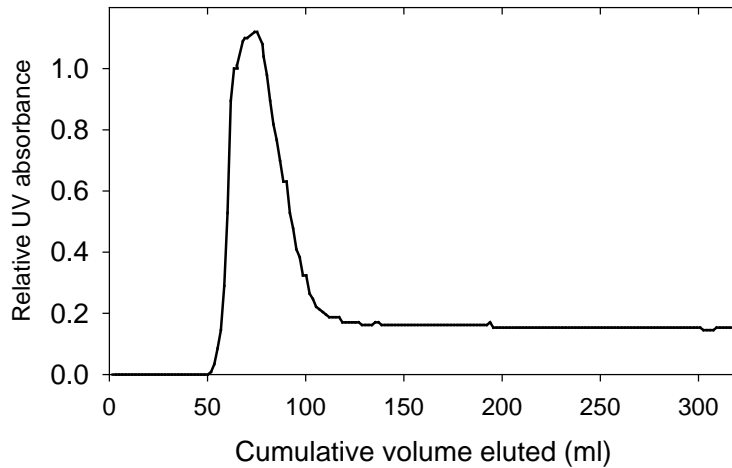


Figure 4-2 Relative UV absorbance vs. cumulative volume eluted from the column for 12 fractions. Maximum absorbance is observed for fractions 2 and 3 according to the elution volumes in Table 4-2.

4.3.2 Repeatability of asphaltene separation on sea sand

The average value of asphaltene recovery percentage and the standard deviation for 5 chromatography separations on sea sand is calculated here:

$$C_{\text{mean}} = \frac{28.59 + 30.23 + 32.00 + 31.70 + 33.36}{5} = 31.17\% \quad (4.3)$$

$$\sigma_c = \left(\frac{(31.17 - 28.59)^2 + (31.17 - 30.23)^2 + (31.17 - 32)^2 + (31.70 - 31.17)^2 + (33.36 - 31.17)^2}{4} \right)^{0.5} = 1.82\%$$

$$C = 31.2 \pm 1.8\% \quad (4.4)$$

Consequently, the chromatographic separations were repeatable to within ± 2 wt%, so that larger differences were considered significant.

4.4 Effect of solvent strength on asphaltene recovery

The effect of solvent strength on asphaltene and metal recovery was studied using three solvents blends with different solubility parameters. The data at the flocculation point were presented above. For comparison, we repeated the separation with pure dichloromethane and a mixture of pentane and methylene chloride above the flocculation point. The solubility parameter of a solvent mixture is defined by the following equation:

$$\delta_{mix} = \frac{\sum x_i V_i \delta_i}{\sum x_i V_i} = \sum v_i \delta_i \quad (4.5)$$

Where δ_i is solubility parameter, χ_i is mol fraction, V_i is molar volume and v_i is volume fraction. The solubility parameter of the solvent mixture used in the chromatographic separations (properties indicated in Table 4-3) is $\delta_{mix} = 17.0 \text{ MPa}^{0.5}$

Table 4-3 Solubility parameter, molar volumes and volume fraction of solvent used in the solvent mixture

Solvent	δ_i (MPa ^{0.5})	v_i (volume fraction)	V_i (molar volume) $\frac{cm^3}{mol}$
Pentane	14.5	0.55	115.3
Dichloromethane	20	0.45	64.07

For an intermediate solvent, in between the flocculation point, we used a blend of 32% pentane/68% dichloromethane (volume/volume). With $v_D=0.68$ and $v_p = 0.32$, the mixture gave a solubility parameter of 18.2 MPa^{1/2} from equation (4.5).

Table 4-4 Asphaltene recovery percentage for three different solubility parameters and volume ratios of pentane-to-dichloromethane in the solvent mixture.

$\frac{V_P}{V_D}$	δ_{mix} (MPa ^{0.5})	Asphaltene Recovery (%)
0.55/0.45	17	31
0.32/0.68	18.2	37
0	20	41

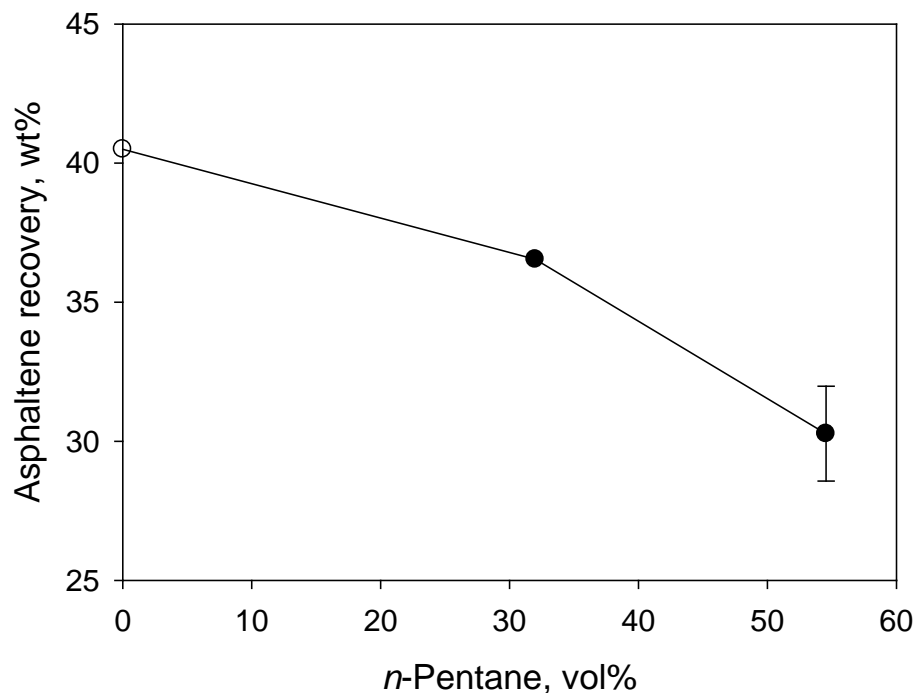


Figure 4-3 Asphaltene recovery percentage vs. volume percentage of pentane in solution

As the volume percentage of pentane in the solvent mixture decreased, or as the solubility parameter of the solvent mixture increased (Table 4-4), the asphaltene recovery percentage increased significantly. The asphaltene adsorption on surface of sea sand was the highest at the flocculation point (the volume ratio of 0.55/0.45 pentane/dichloromethane). This result is in agreement with Castillo et al. (2001) who concluded that the less soluble asphaltene which tended to aggregate in solution, also tended to adsorb on mineral surfaces from toluene solutions. Even with pure dichloromethane, 60% of the asphaltene was still retained on the surface of chromatography packing (Figure 4-3).

4.5 Fluorescence spectra of Cold Lake asphaltenes separated on sea sand

Three different solvent mixtures with three different solubility parameters were prepared for chromatography separations using sea sand as chromatography packing, as described in section 4.4. Fluorescence spectroscopy analysis was done on all 12 collected fractions. As shown in Figure 4-4, a significant shift of peak intensity in the fluorescence emission spectrum was observed when a solvent mixture with a solubility parameter of $17.0 \text{ MPa}^{0.5}$ was used. These shifts in emission from 440nm to 490 nm accounted for the visual observation of differences in color between the eluted fractions. (Table 4-5)

Table 4-5 Maximum peak intensities and wavelengths for fractions 2-5

Fraction volume(ml)	mg recovered	λ_{max} (nm)	I (A.U)
54	10.5	490	290
81	4.5	490	300
108	1.4	440	900
135	0.2	440	750

No shifts of peak intensity in the fluorescence emission spectrum were achieved when solvent mixtures with higher solubility parameters were used. This result was an indication of poor selectivity based on shifts of peak intensity in the fluorescence

emission spectra. Similarly, there was no distinct difference in the observed color of the eluted fractions.

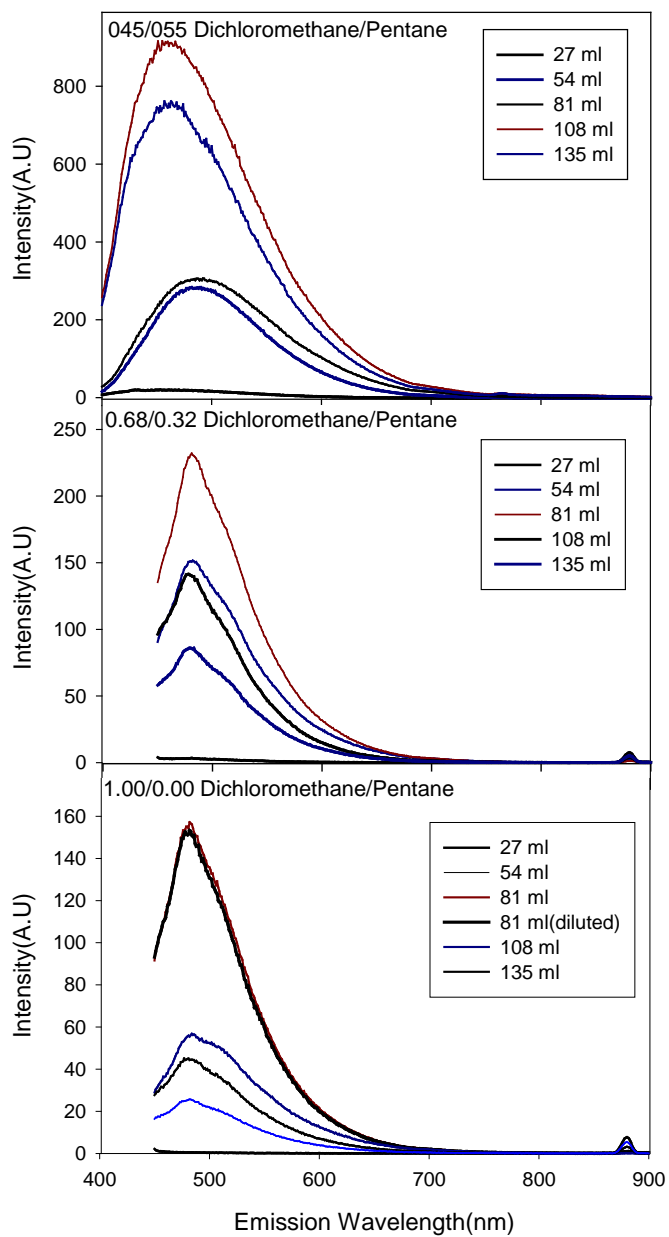


Figure 4-4 Fluorescence of five different fractions eluted from the column for three different solvent mixtures using sea sand as chromatography packing. An excitation wavelength of 440 nm was selected for all three experiments

All the fractions of asphaltenes are complex mixtures and a change in the solubility parameter retains material on the column, which allows us to see color. When the material is not retained, no color difference is observed.

4.6 Sea Sand treated with acid and base

Sea sand was washed with acid and base to investigate the role of surface chemistry on asphaltene separation. These treatments would remove trace elements, such as iron, alkali metals, and alkaline earth metals, from the silica surface.

As shown in Table 4-5, treating sea sand with acid and base did not affect the recovery of asphaltene, within experimental error, but gave poor selectivity based on shifts of peak intensity in the fluorescence emission spectra. (Figure 4-5).

Table 4-6 Recovery of asphaltenes from for sea sand washed with acid and base, using a solvent mixture with a solubility parameter of 17.0 MPa^{0.5}

Packing	Untreated sea sand	sand NaOH treated	sand HCl treated
Recovery (%)	31 ± 2 %	29 %	32 %

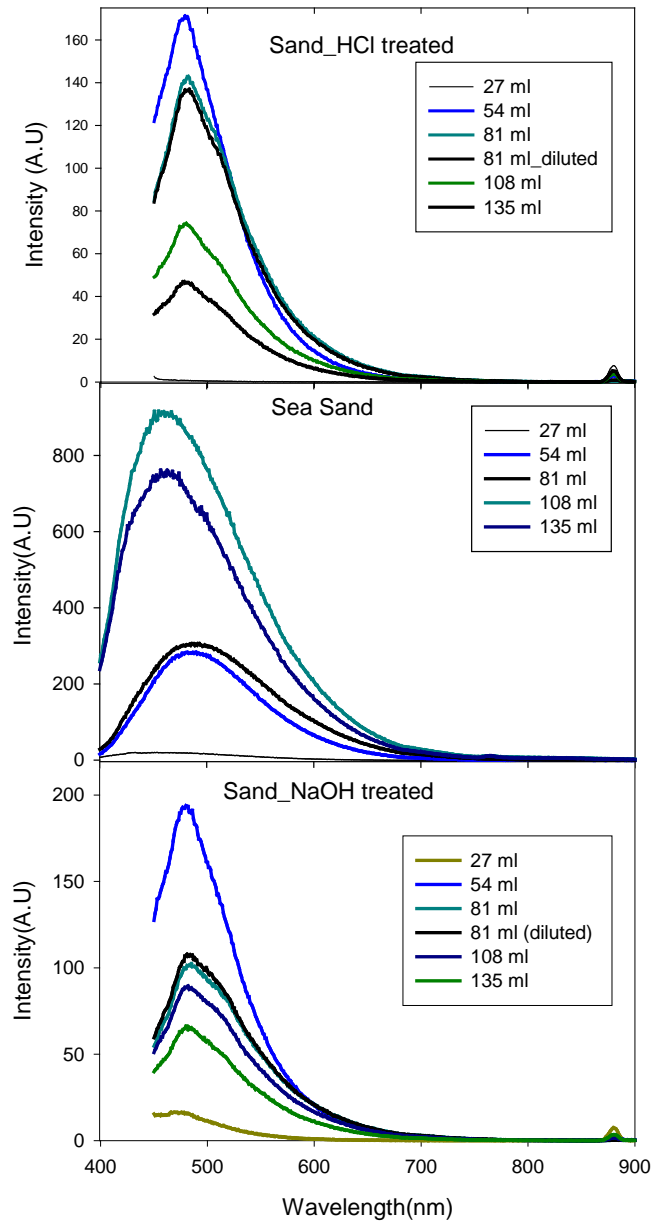


Figure 4-5 Fluorescence spectra of five fractions from sea sand, sand acid treated and sand base treated at the flocculation onset condition. An excitation wavelength of 440 nm was selected for all three cases.

Treating sea sand with acid and base results in poor selectivity based on shifts of peak intensity in the fluorescence emission spectra. The silanol groups are known for having

the characteristics of both acid and base (amphoteric characteristic) and have a tendency to react with both strong acids like HCl and strong bases like NaOH. Therefore, it is likely that the silanol groups on the surface of silica sand are less active when sea sand is treated with acid and base. In this case, the solvent-asphaltene interactions dominate the surface-asphaltene interactions in the case of less active silanol groups on the surface which results in poor selectivity based on shifts of peak intensity in the fluorescence emission spectra. Another reason for the lack of selectivity would be due to the removal of trace metals from the surface of sea sand after treatment with acid and base. The quantities of these metals are shown in Table 4-7.

Table 4-7 Atomic concentrations of different components on the surface of sea sand according to XPS.

Component	Atomic concentration%
Na	0.16
Fe	1.48
O	56.77
Ti	0.12
N	0.34
K	0.36
Ca	0.19
C	17.89
Si	18.12
Al	4.58

4.7 Separation of Vanadium

The vanadium concentration in the collected fractions was reported in parts per million by mass (ppmw). Cold Lake asphaltenes contain 850 ppmw vanadium. This value is multiplied by the mass of asphaltene used originally for separations (circa 59 mg) in order to obtain the amount of vanadium in each sample in μg . The vanadium recovery fraction was calculated according to the following equation:

$$\text{Recovery percentage in fraction "n"} = \frac{\sum_1^n \text{vanadium in fraction } (\mu\text{g})}{\text{vanadium in asphaltene sample } (\mu\text{g})} \times 100 \quad (4.8)$$

$$\text{Vanadium concentraton}(\mu\text{g}) = \text{vanadium concentration}(\text{ppm}) \times 50 \quad (4.9)$$

4.7.1 Repeatability of vanadium separations on sea sand

$$C = \frac{5.2 + 5.1 + 8.6}{3} = 6.3\% \quad (4.10)$$

$$\delta c = \left(\frac{(6.3 - 5.2)^2 + (6.3 - 5.1)^2 + (6.3 - 8.6)^2}{2} \right)^{0.5} = 2.0\%$$

$$C = 6.3 \pm 2.0 \% \quad (4.11)$$

Consequently, the experimental error for the metal recovery percentages was ± 2 wt%, so that larger differences were considered significant

4.7.2 Vanadium recovery in chromatographic fractions

The samples collected from chromatography separations with two different solvent mixtures were analyzed for vanadium concentration after acid digestion using Inductive Coupled Plasma technique. The results for the cumulative vanadium recovery percentages are shown in Table 4-8.

Table 4-8 Asphaltene and metal recovery percentage for two different solubility parameters of solvent mixture (pentane and DCM).

Solvent ratio, $\frac{v_P}{v_D}$	Solubility parameter MPa ^{0.5}	Asphaltene recovery (%)	Metal recovery (%)
$\frac{0.55}{0.45}$	17.0	31 ± 2	6 ± 2%
$\frac{0.32}{0.68}$	18.2	37	16

Figure 4-6 and Figure 4-7 represent the cumulative recovery of metal and asphaltene in fractions 1-11 for two different solubility parameters in the solvent mixture. The UV absorbance in these figures indicates that maximum absorbance is achieved for fractions 2 and 3 which have higher mass of material compared to the rest of the fractions.

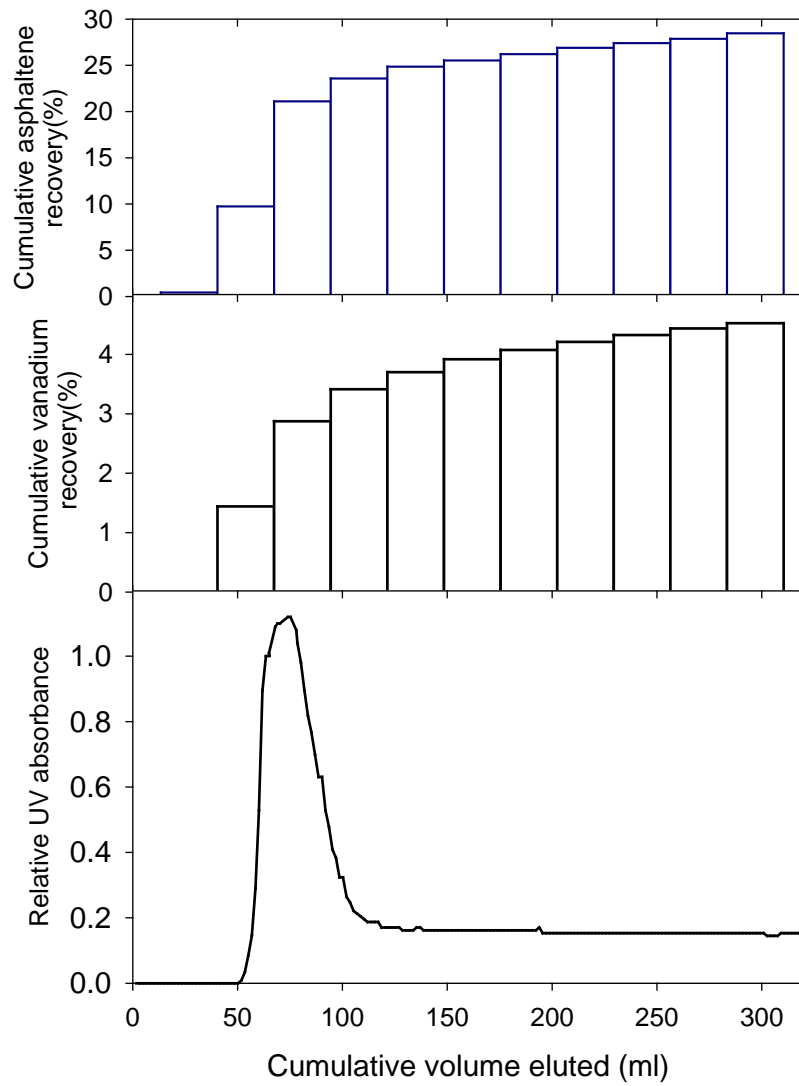


Figure 4-6 Cumulative asphaltene and metal recovery percentage at a solubility parameter of $17.0 \text{ MPa}^{0.5}$ for solvent mixture.

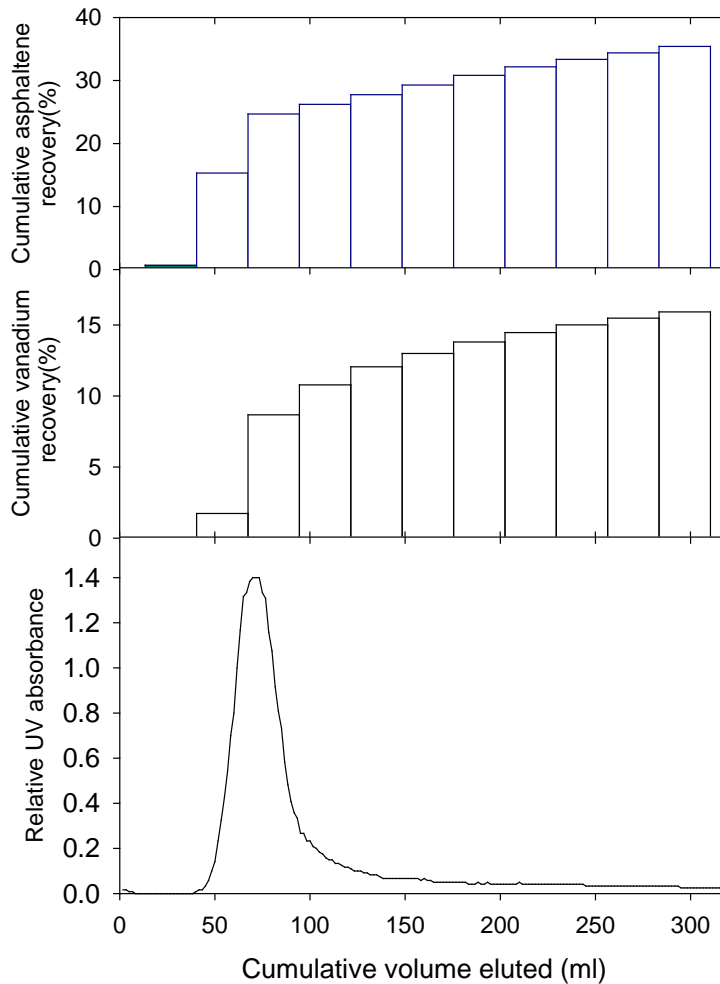


Figure 4-7 Cumulative asphaltene and metal recovery percentage at a solubility parameter of 18.2 MPa^{0.5}

As shown in Table 4-8, both the asphaltene and vanadium recovery percentages increase with an increase in the solubility parameter of the solvent mixture. The change in vanadium recovery was much more significant than the change in total asphaltene recovery, indicating that metal bearing species were interacting more strongly with the solid phase at the lower solvent strength (lower value of δ). (Spiecker et al. 2003) who have studied asphaltene aggregation and solubility behavior in solution. They concluded that a particular sub fraction with lower H/C ratio (higher aromaticity) has modestly

higher V, N, Ni and Fe contents than the other fractions of the asphaltenes. Such a non-aggregated fraction could be responsible for the interactions with the sand during chromatography. In strong solvent, this material would be eluted more easily, either due to displacement from the surface by adsorption of solvent or due to enhanced solubility. The bulk of the vanadium was associated with the retained asphaltenes at both solvent strengths, accounting for at least 84% of the vanadium. A very similar pattern of asphaltene and vanadium elution in Figure 4-8 and Figure 4-9 was observed.

4.8 Effect of column temperature

As discussed in Chapter 2, asphaltene solutions contain aggregates of order 5 nm diameter even in strong solvents such as toluene. This aggregation behavior would interfere with selective chromatography of molecular species because groups of molecules would interact with the surface simultaneously, rather than individual components. The degree of aggregation declines with temperature, therefore, the chromatographic separation was repeated at 50°C. The mixture of pentane and dichloromethane was too volatile for use at this temperature, therefore, a mixture of toluene and hexane was used instead.

A solubility parameter of 16.9 MPa^{0.5} was obtained when values of $\nu_h = 0.4$ and $\nu_t = 0.6$ and solubility parameters for toluene and hexane were substituted in equation (4.5). Since selective separation based on the shifts of peak intensity in the fluorescence emission spectra and difference in colors for each fraction was achieved with separations at the

flocculation point, the solubility parameter of the solvent mixture at the flocculation point was chosen for calculations of toluene-to-hexane volume ratios. The ratio selected for toluene/hexane mixture was 0.6/0.4 on a volume basis.

According to Figure 4-8 and Figure 4-9, two peak intensities at 460 nm and approximately 500 nm were observed in the fluorescence emission spectra of each fraction for experiments performed at room temperature and at 50. No significant changes were observed in the fluorescence emission spectra when temperature was increased from room temperature to 30 using the same solvent mixture. Selective separation was not observed for toluene/hexane solution based on the fluorescence spectra and lack of color difference in the eluted fractions. It is likely that at elevated temperatures, the degree of aggregation decreases but also the solvent-asphaltene interactions are more significant rather than asphaltene-surface interactions which results in more asphaltene recovery and less selectivity.

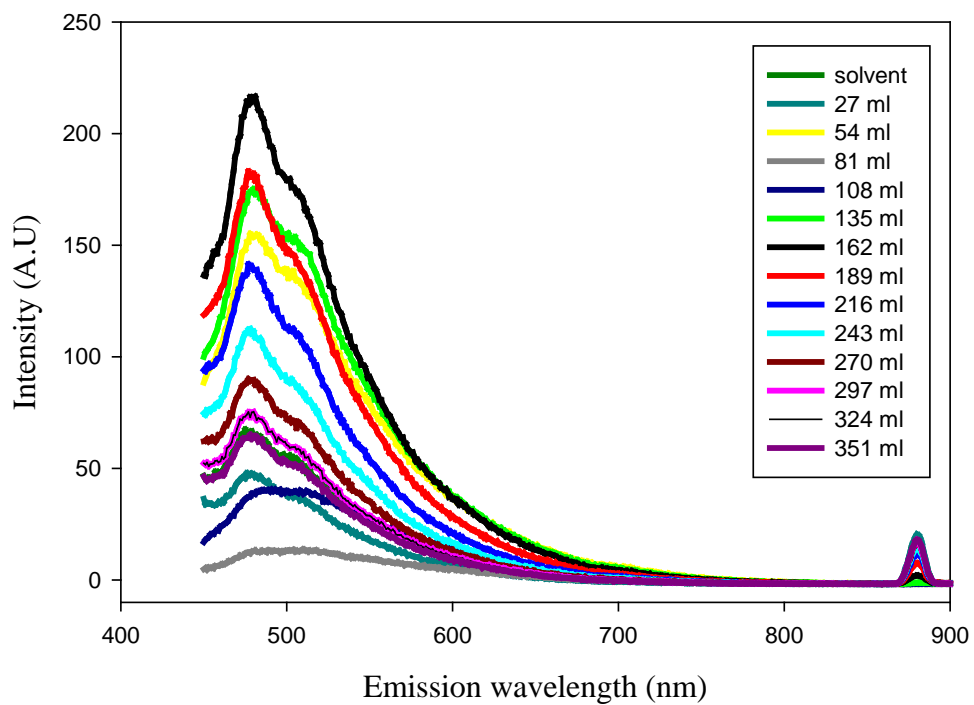


Figure 4-8 Fluorescence spectra of 12 fractions eluted from the column at room temperature. An excitation wavelength of 440 nm was selected for toluene/hexane mixture at room temperature.

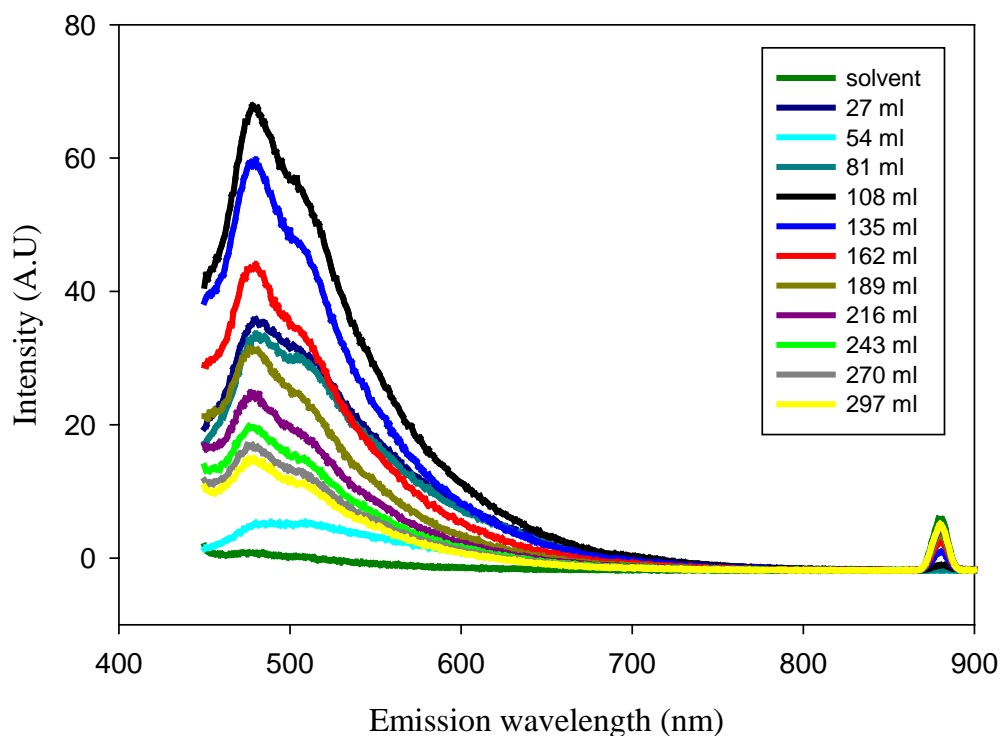


Figure 4-9 Fluorescence spectra of 12 fractions eluted from the column at 50°C temperature. An excitation wavelength of 440 nm was selected analysis of solutions in hexane/toluene at room temperature.

The data for asphaltene recovery from the column are consistent with strong attachment of aggregates to the surface of the column at all solvent strengths. In order to reduce aggregation of the asphaltenes, the column temperature was increased to ~ 50°C and the collected fractions from the column operating at the specific temperature were analyzed for vanadium concentration using ICP technique. The results are shown in Table 4-9.

Table 4-9 Metal and asphaltene recovery percentages for a solvent mixture of toluene / hexane at two different temperatures.

Temperature °C	Solubility parameter (MPa ^{0.5})	Metal recovery percentage (%)	Asphaltene recovery percentage (%)
T= 25°C	16.81	50%	40%
T=50°C	16.81	62%	55%

As shown in Table 4-9, asphaltene adsorption decreased as the temperature of the column increased. This result is in complete agreement with Abdallah and Taylor (2007) who studied surface characterization of adsorbed asphaltene on a stainless steel surface. They studied the effect of temperature on C₇-asphaltene adsorption on a steel surface at three different temperatures (22, 40 and 60°C). In their study, asphaltene adsorption was the highest at 22 °C.

The recovery of vanadium compounds increased as the temperature increased from 25°C to 50°C. As the temperature increased, the interactions between solid phase and asphaltenes decrease which results in less interaction between the vanadium bearing compounds and solid phase as well. Therefore, the metal recovery percentage increases.

4.9 Discussion

The recovery of asphaltenes from the columns increased with the strength of the solvent, but resulted in less intense peaks from fluorescence spectroscopy, and a loss of selectivity of separation based on shifts in peak intensity. Similarly, the stronger solvent blends gave higher values of vanadium recovery percentage. This study suggests that the selectivity of the separation is highest when the asphaltenes are close to the flocculation point, which also gives more retention on the packing. A distinct difference between the fraction colors indicated elution of different compounds and selective separation at the flocculation point which could not be observed when pure dichloromethane is used for separations. There was no evidence that the color indicated a high concentration of V in any fraction. The color could be due to removal of the vanadium, or separation of other fluorophores.

Asphaltene aggregates present in all cases likely accounted for bulk of asphaltene retention. At the flocculation point, asphaltenes have the highest tendency to form aggregates in solution which results in more retention of the asphaltenes. With pure dichloromethane, the tendency for aggregation in solution decreases which results in less retention of the asphaltenes on the chromatography packing. Also, it is likely that less tendency to form aggregates at the flocculation point, results in less retention of metals on the surface of chromatography packing and an increase in metal recovery.

Silica material with functional groups which form very stable and strong chemical bonds with only metal compounds in the asphaltene mixture might be better packings for

separation of metal compounds from asphaltenes. Detailed knowledge about the forms of metal compounds, their chemical property and also mechanism of interactions between metal bearing compounds and proposed ligands on the surface of silica material is required to develop better packings for separation of metal bearing compounds.

In our study we treated silica powder with different reactants to investigate the effect of surface chemistry on asphaltene and metal recovery. The results for different silica materials and their hydrothermal treatment, is discussed in the next chapter.

4.10 Conclusions

According to our study, asphaltene separation was achieved on sea sand with flash chromatography technique based on the color difference in fractions and the fluorescence emission spectra. The scaling of separations between open column and flash chromatography were successful which results in less time and solvent usage for each separation .Using sea sand as chromatography packing is beneficial because it is considered as an inexpensive and abundant silica material .

4.11 References

1. Abdallah, W. A. and S. D. Taylor (2007). "Surface characterization of adsorbed asphaltene on a stainless steel surface." Nuclear Instruments and Methods in Physics Research, Section B: Beam Interactions with Materials and Atoms **258**(1): 213-217.
2. Buckley, J. S. and Y. Liu (1998). "Some mechanisms of crude oil/brine/solid interactions." Journal of Petroleum Science and Engineering **20**(3-4): 155-160.
3. Castillo, J., A. Fernández, et al. (2001). "New techniques and methods for the study of aggregation, adsorption, and solubility of asphaltenes. Impact of these properties on colloidal structure and flocculation." Petroleum Science and Technology **19**(1-2): 75-106.
4. Spiecker, P. M., K. L. Gawrys, et al. (2003). "Aggregation and solubility behavior of asphaltenes and their subfractions." Journal of Colloid and Interface Science **267**(1): 178-193.

Chapter 5

Separation on modified silica materials

5.1 Introduction

Our hypothesis for the modifications to the silica packings was that an increase in the asphaltene recovery percentage would be achieved by providing fewer active sites on the surface of modified silica material. Silica packing materials were prepared by treating with different alkaline earth metals (in collaboration with with Dr.Kuznicki's group). Chromatographic behavior was determined under a standard set of conditions of flow and solvent composition. The hydrothermal treatment procedure for preparation of the silica is explained in section 5.2. FTIR spectroscopy and XPS were used for surface characterization of the different silica materials.

5.2 Hydrothermal treatment of silica

Plastic disposable sample weigh dishes were filled each half way with colloidal silica (Silica HS-40, colloidal silica, 40 wt% suspension in water, Sigma-Aldrich CHEMIE, Steinheim, Germany), and left in an oven at 80°C overnight (Each tray yielded ~50g). The resulting solid was ground to give a silica powder of 20-50 mesh. Approximately 300 g was placed in the oven at 150°C for three hours. One liter of H₂O was poured into a large glass beaker and brought to 50°C. The required amount of alkaline earth metal reactant and 100 g of silica powder were added into the glass beaker and stirred for one

hour (Table 5-1). After reaction, the contents were vacuum filtered and placed in a container for drying overnight at 80°C.

Dichloromethane, pentane and nitric acid with the same catalog number mentioned in chapter 3 were used in this set of experiments using modified silica as chromatography packing. The same Cold Lake asphaltene sample was used as in Chapter3.

Table 5-1 Hydrothermal treatment conditions for modification of silica

Sample	Temperature (°C)	Reactant	Amount of Reactant*(mol)
1	150	N/A	0.25
2	150	MgCl ₂ -6H ₂ O	0.25
3	150	CaO	0.25
4	150	Ba (OH) ₂	0.25
5	150	Sr (OH) ₂	0.25

*14 g of CaO was used for 250 g of silica which corresponds to 0.25 mol of reactant.

This amount was applied for all reactants to apply a constant mol concentration.

The chromatographic separation was the same as described in Chapter 4, except that all fractions were added together for acid digestion and ICP analysis for metals content.

5.3 Results & Discussion

5.3.1 Recovery of Cold Lake asphaltenes from different silica materials

The recoveries of asphaltene from the modified silica packings are listed in Table 5-2.

Table 5-2 Cold Lake asphaltene recovery percentage from 5 different silica materials

Sample	Reactant	Recovery%
1	None	33 ± 2
2	MgCl ₂ ·6H ₂ O	37
3	CaO	37
4	Ba(OH) ₂	44
5	Sr(OH) ₂	39

As shown in Table 5-2, there was some change in the recovery percentage of the material eluted from the column when 4 different types of silica material are used as a chromatography packing. Given a repeatability of +/- 2%, the recovery was significantly higher for the barium-treated silica.

5.3.2 Metal recovery percentage from different silica materials

The cumulative metal recovery percentages were calculated after combining fractions 1-12 and measuring the metal concentration in the combined mixture using ICP analysis.

The results are introduced in Figure 5-2 for 5 different types of silica material used as a chromatography packing.

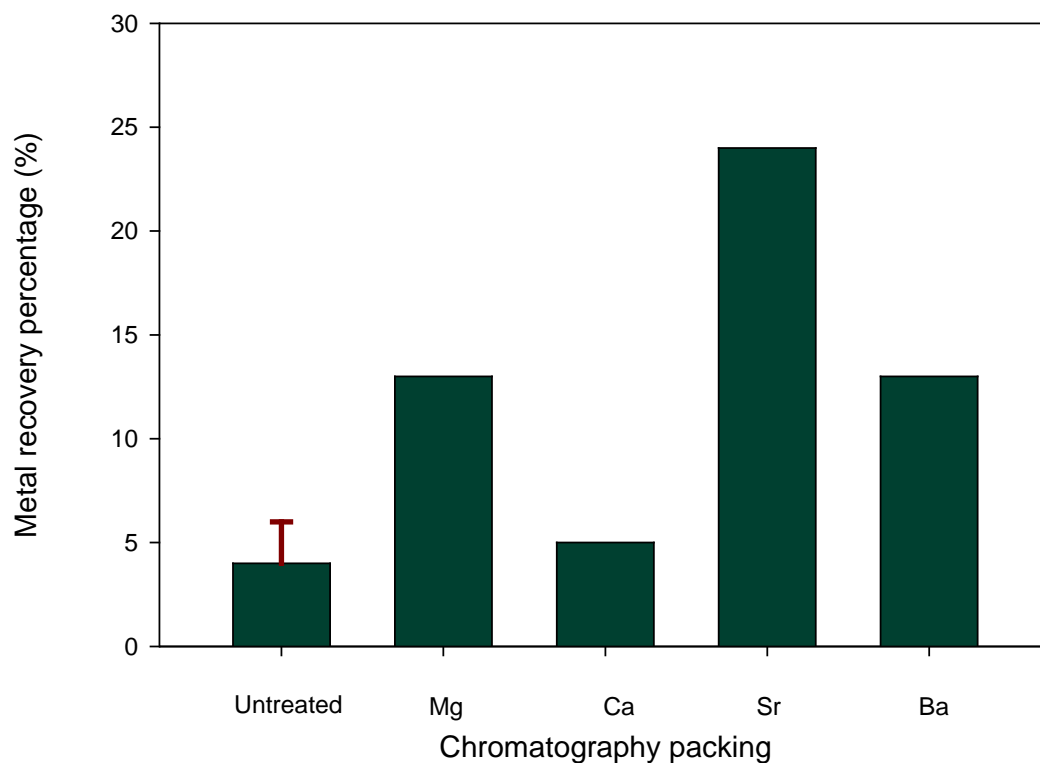


Figure 5-1 Metal recovery percentage of alkaline earth metal modified silica materials used as a chromatography packing. A volume ration of 0.55/0.45 of pentane/dichloromethane was used as a solvent mixture.

The ranking of metal recovery following comments on treated silica was in the series:

untreated ~ Ca < Ba ~ Mg < Sr.

Ikoma et al. (2001) examined the adsorption behavior of different silica-metal oxide particles for different type of basic components. According to their observations, it is likely that the treatment of silica materials with different metal ions decreases the activity of silanol groups on the surface which results in elution of basic compounds when the treated silica materials are used as a chromatography packing. In our study, treating silica with different metal ions results in an increase in metal recovery percentage as shown in Figure 5-1.

5.3.3 Surface characterization results

5.3.3.1 FTIR Spectroscopy results

Raw material and metal treated silica were ground to a fine powder and kept under vacuum at 150 °C for 2 days. Samples were cooled to room temperature and 10 mg of sample was placed on ZnSe crystal for IR analysis. FTIR characterization was performed to characterize the surface of silica materials before and after hydrothermal treatment. Our goal was to compare the surface of different silica materials used as chromatography packing, in order to explain the differences in metal and asphaltene recoveries for these materials. For this purpose, wavelengths between 700nm-1100nm were selected from the full range of the spectra and the absorbance within the selected wavelengths for each treated silica material were adjusted to obtain the absorbance of a strong silica band at 1100 cm^{-1} (Figure 5-2).

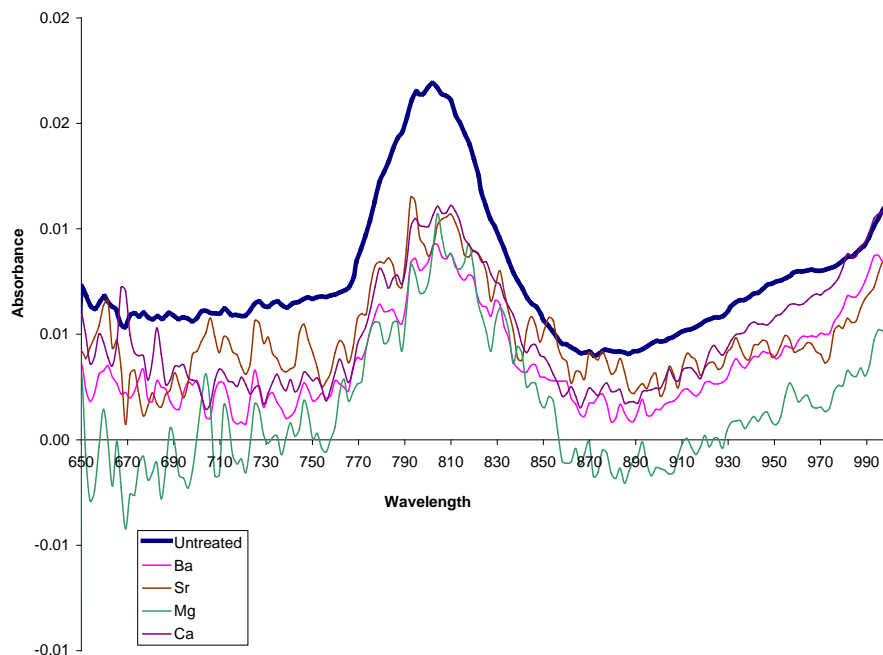


Figure 5-2 FTIR plots for five different silica materials used as chromatography packing. The spectra were scaled to give the same offset between the plots.

According to Figure 5-2, a weak shoulder is observed at a wavelength of 960 cm^{-1} in the blue plot which corresponds to the SiOH stretching vibrations for untreated silica. This shoulder is not observed for treated silica samples. This result implies that the hydrothermal treatment changed the surface, but it does not discriminate between the treated samples.

5.3.3.2 XPS results

Although the treatment of the silica powders was designed to expose the surface to the same molar concentration of cation, this does not guarantee that the same extent of surface reaction on the surface of treated materials. XPS was used to examine the surface composition of the samples to assess the extent of surface modification.

Table 5-3 Atomic concentration ratios on surface of 5 different silica materials

Sample	Reactant	Atomic ratio of added cation to Si
1	N/A	0
2	MgCl ₂ -6H ₂ O	0.017
3	CaO	0.045
4	Ba(OH) ₂	0.17
5	Sr(OH) ₂	0.11

An increase in the metal/Si ratio when silica was treated with different metal ions confirmed significant changes in surface composition due to the hydrothermal treatment. Addition of the alkaline earth metals to the silica surface would destroy or block the surface silanol groups. According to Table 5-3, the Ba treated sample would have the fewest active sites for adsorption of the asphaltenes due to highest metal/Si ratio on the surface. Figure 5-3 shows a plot of recovery of asphaltene and vanadium versus surface concentration of added cation. The asphaltene recovery showed a monotonic increase with surface substitution, consistent with a role for silanol groups in retaining the asphaltenes on the surface of the packings.

The vanadium recoveries increased much more dramatically, to a maximum with Sr, then a lower value with Ba. The lack of a clear trend of vanadium recovery with surface coverage suggests that other factors than silanol concentration influence the recovery of the metals. For example, the recovery of vanadium increased with the size of the ions, rather than the surface concentration.

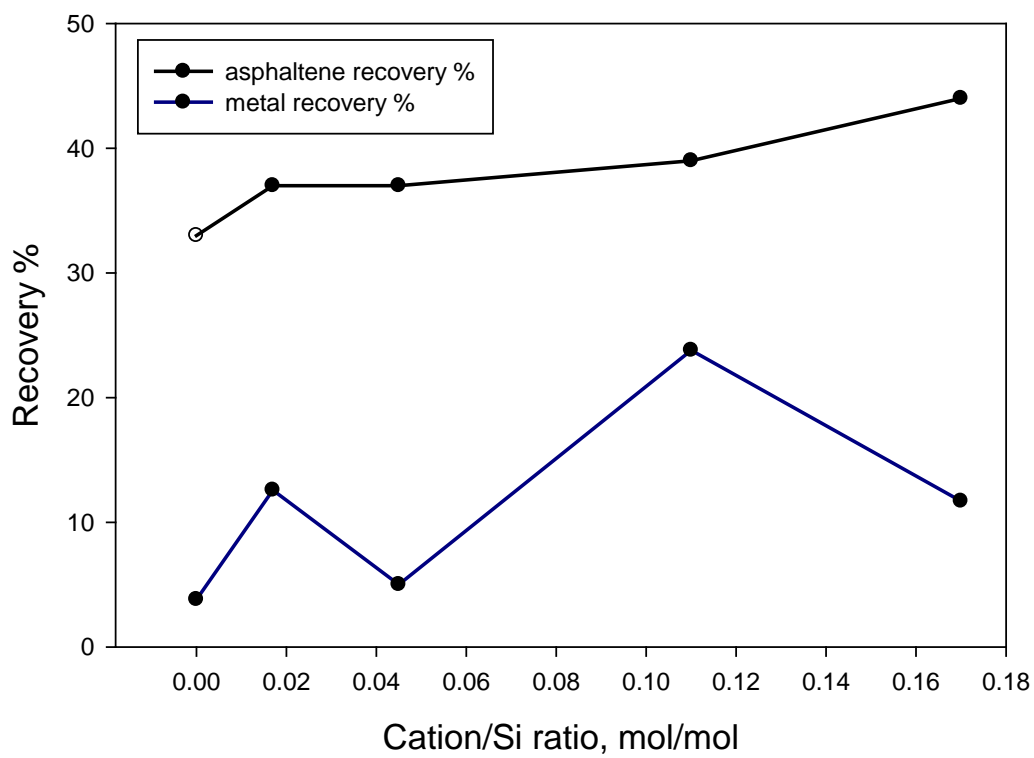


Figure 5-3 plot of recovery of asphaltene and vanadium versus surface concentration of added cation.

5.3.4 Fluorescence spectra of Cold Lake asphaltenes from treated silica materials

Fluorescence emission spectra of 5 different silica materials are presented in Figure 5-4 to Figure 5-8. A single excitation wavelength of 440 nm again was selected here for each case. The solvent mixture which was used for chromatography separations was 0.55/0.45 pentane-to-dichloromethane.

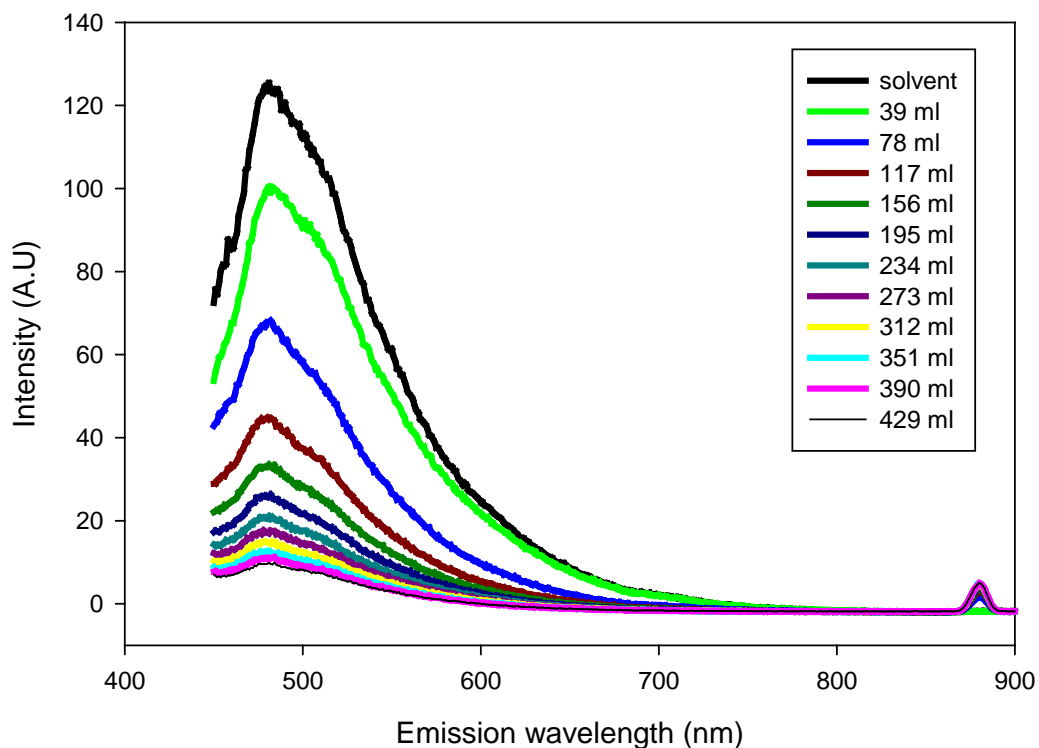


Figure 5-4 Fluorescence spectra of 12 fractions from silica (untreated)

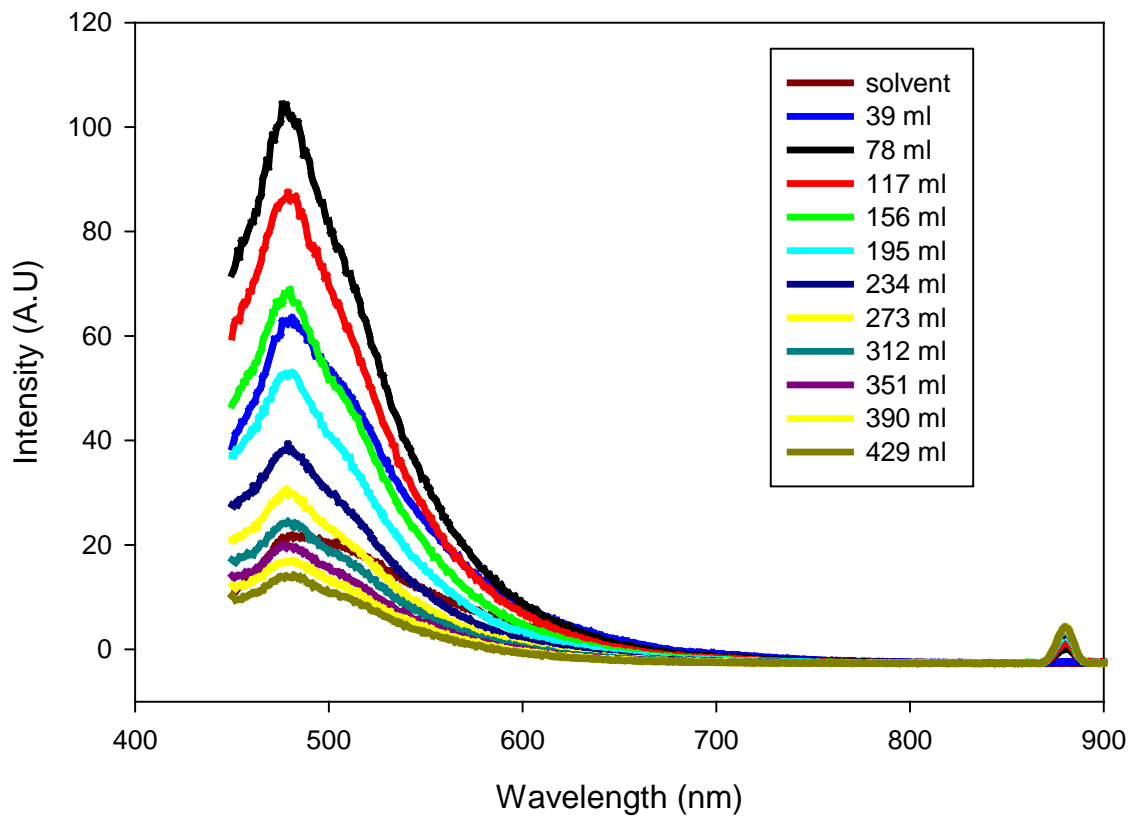


Figure 5-5 Fluorescence spectra of 12 fractions from silica treated with Mg.

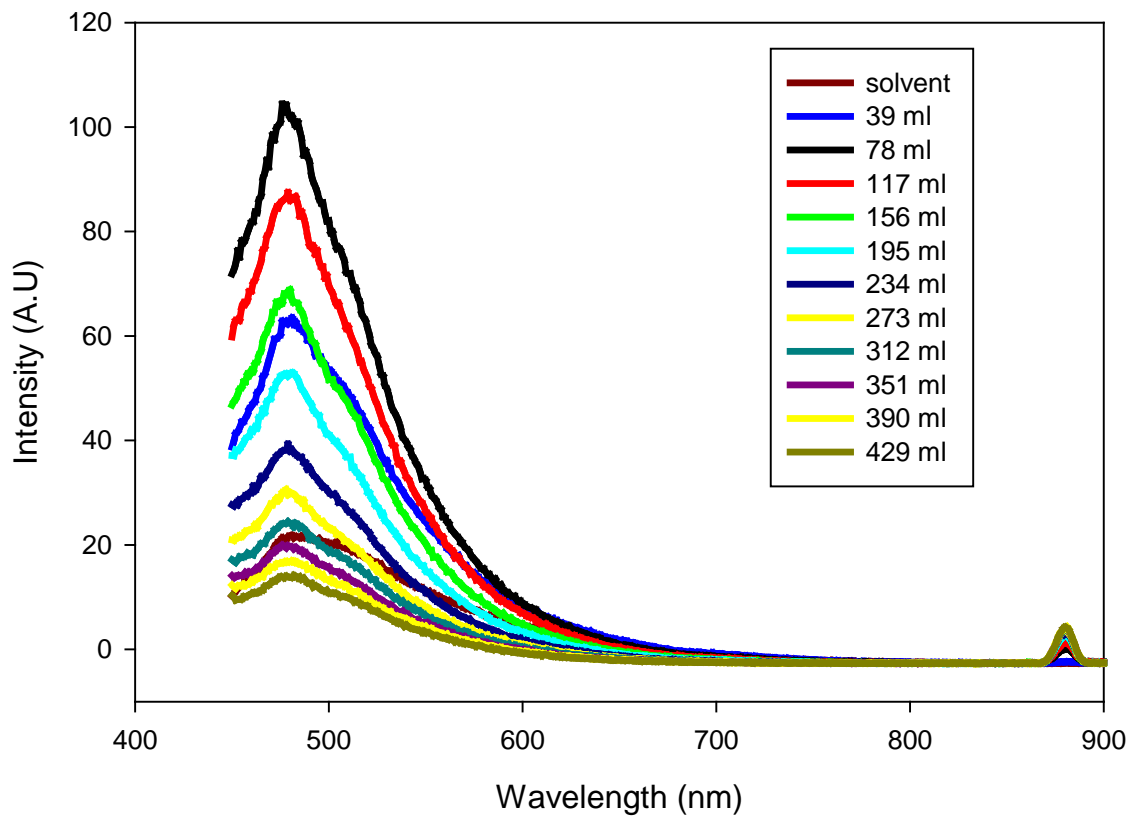


Figure 5-6 Fluorescence spectra of 12 fractions from Silica treated with Ca

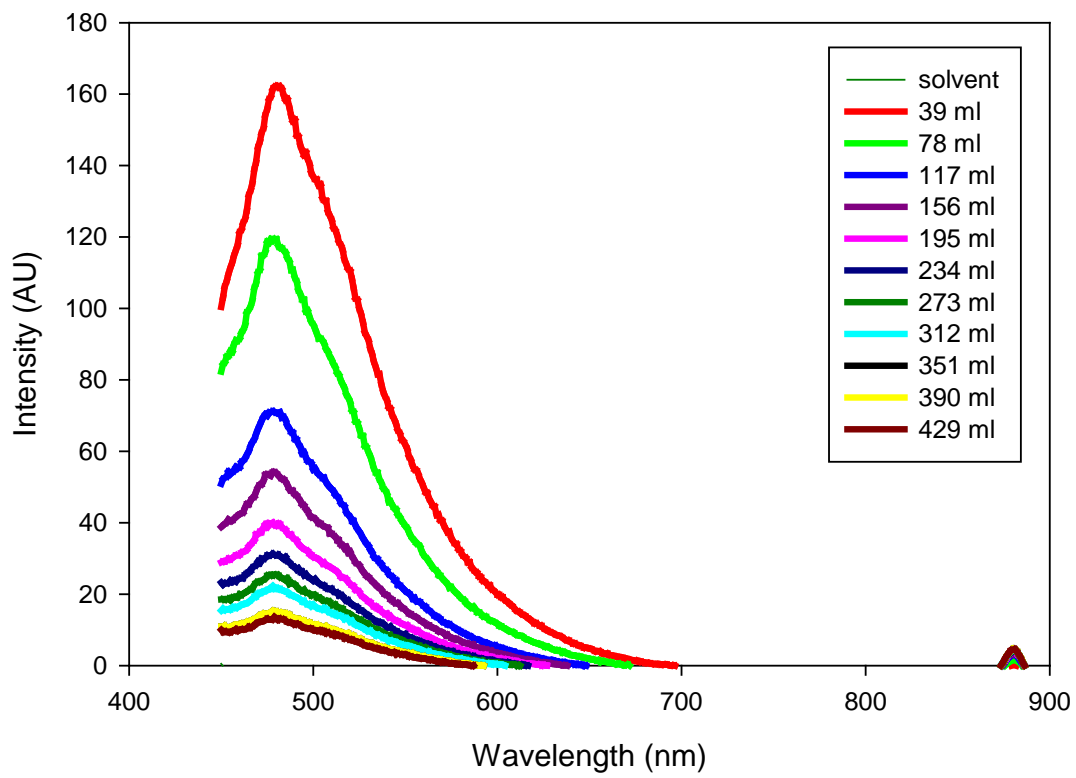


Figure 5-7 Fluorescence spectra of 12 fractions from silica treated with Ba .

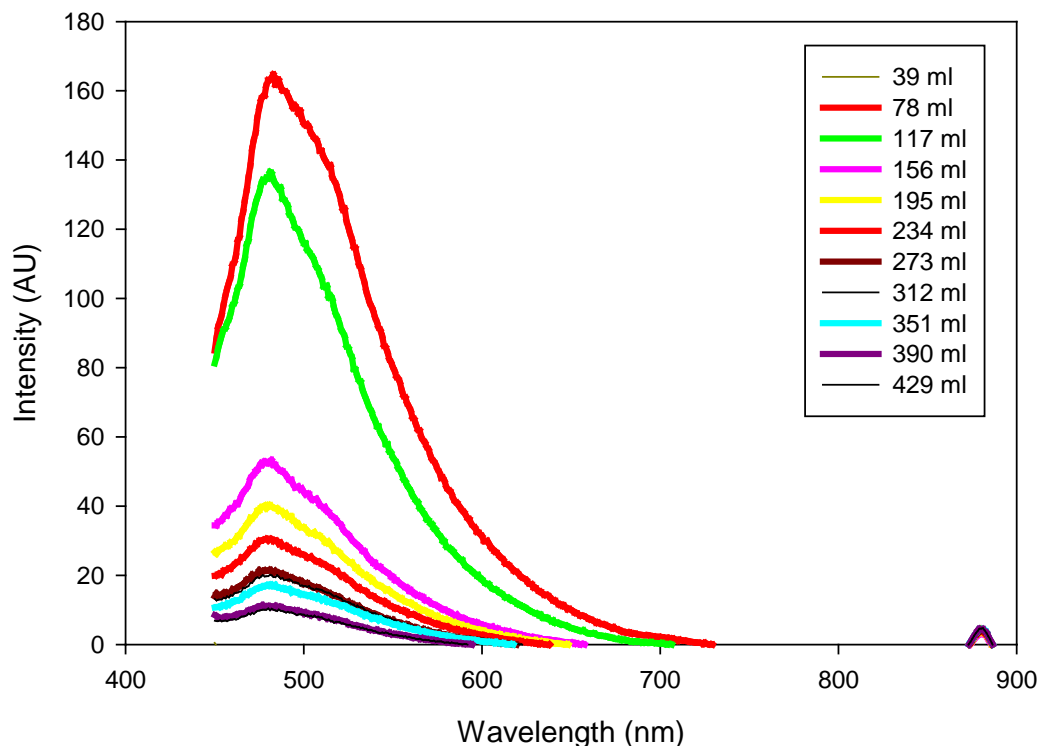


Figure 5-8 Fluorescence spectra of 12 fractions from Silica treated with Sr.

The fluorescence plots of all 5 types of silica material are the same. No shift in peak intensity in the fluorescence emission spectra was observed when silica treated with different types of reactants is used as a chromatography packing. As mentioned in chapter 3, shifts of peak intensity in the fluorescence emission spectra were observed for untreated sea sand. According to fluorescence results for untreated sea sand and different silica materials, selective separation is achieved when untreated sea sand was used as a chromatography packing. One explanation for the selectivity achieved for sea sand, is that the trace elements, such as iron, alkali metals, and alkaline earth metals on the silica

surface interact with free asphaltene molecules which are not within the aggregated molecules and selectivity is achieved when sea sand is used as a chromatography packing. In our study, we designed novel silica materials to attempt selective separation of metals from asphaltenes, which can be used as an inexpensive replacement for conventional chromatography. We were able to retain more than 70% of the metals on the surface which is favorable for separation of metal compounds from asphaltenes. The treatment with alkali earth metals did not improve the vanadium retention on the surface and the metal recovery percentage increased when the metal/Si ratio increased on the surface after treatment. With the silica materials discussed in this chapter, asphaltene recovery percentage increased from 30% for sea and to 44 % for the treated silica materials. Still, the treated silica materials used in our study retained approximately 60% of asphaltene on the surface of silica materials.

Better understanding of the type and nature of interactions of silanol groups and metal bearing compounds within the asphaltenes could lead to developing specific types of silica materials which would retain less asphaltenes and more metals on the surface which is favorable for metal separation.

5.4 Conclusions

Selective separation was not obtained for different silica materials discussed specifically in this chapter according to their fluorescence spectroscopy results, and no color difference was observed for fractions 1-12. The hydrothermal treatment decreased the

retention of the vanadium compounds but resulted in an increase in the asphaltene recovery percentage from 30% for sea sand to 44% for Ba treated silica.

5.5 References

1. Buckley, J. S. and Y. Liu (1998). "Some mechanisms of crude oil/brine/solid interactions." Journal of Petroleum Science and Engineering **20**(3-4): 155-160.
2. Ikoma, S., K. Nobuhara, et al. (2001). Surface properties of silica-titania and silica-zirconia mixed oxide gels. Studies in Surface Science and Catalysis. **132**: 765-768.

Chapter 6

General discussions & Conclusions

In experiments with sea sand and different silica materials treated with alkaline earth metals we understand that aggregated asphaltenes dominate the interactions between the surface of silica materials and asphaltenes which is a result of 60%-70% retention of the asphaltenes on the surface of silica materials. Also, up to 25% of the vanadium compounds may interact with the surface. These compounds are retained at low solubility parameters of the solvent mixture and at high OH concentrations on silica materials. The origin of the shifts of peak intensity in the fluorescence emission spectra requires further study.

Chapter 7 Appendix A

7.1 FTIR results for surface characterization

The blue plots in Figure 7-1 to Figure 7-4 belong to Ludox and the red plot belongs to Ludox treated with 4 different types of reactants. A portion of the spectra (700 cm^{-1} - 1100 cm^{-1}) was necessary to compare Ludox (raw material) with hydrothermally treated Ludox materials as discussed in the result and discussion section in chapter 5. Further conclusion can not be extracted from the FTIR plots for wavelengths in the region of 1100 cm^{-1} - 3000 cm^{-1} .

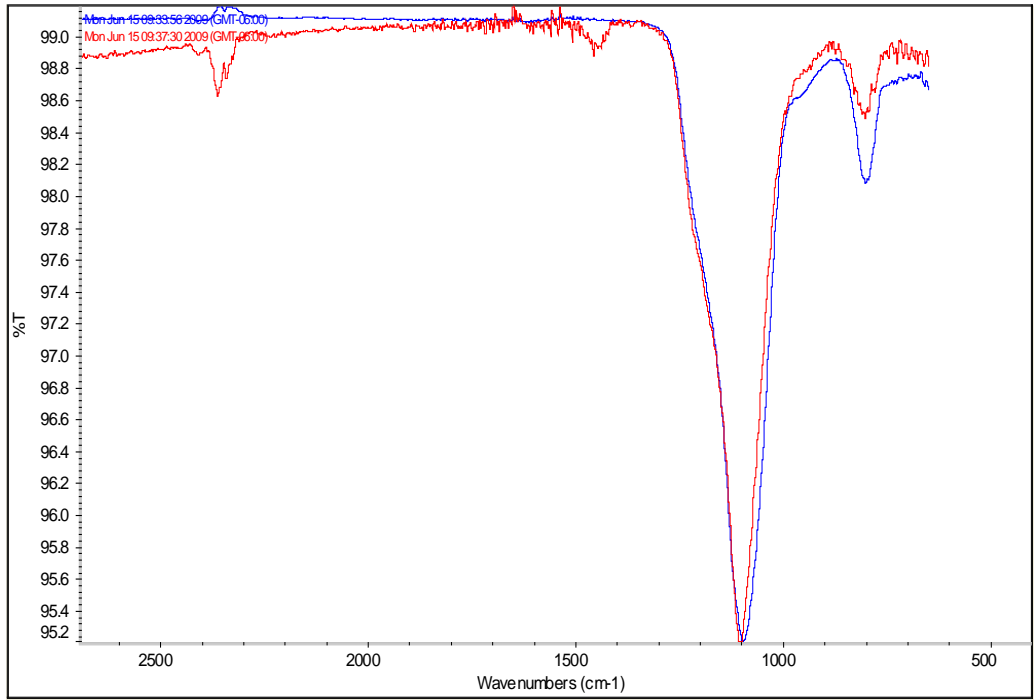


Figure 7-1 FTIR plots for Ludox treated with Ba ions

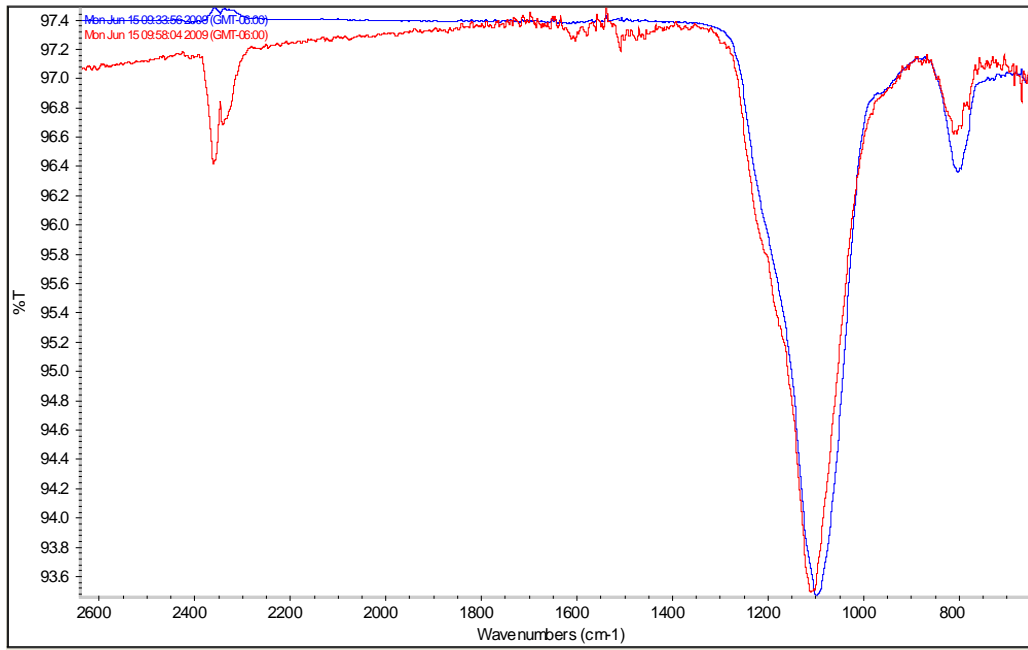


Figure 7-2 FTIR plots for Ludox treated with Ca ions

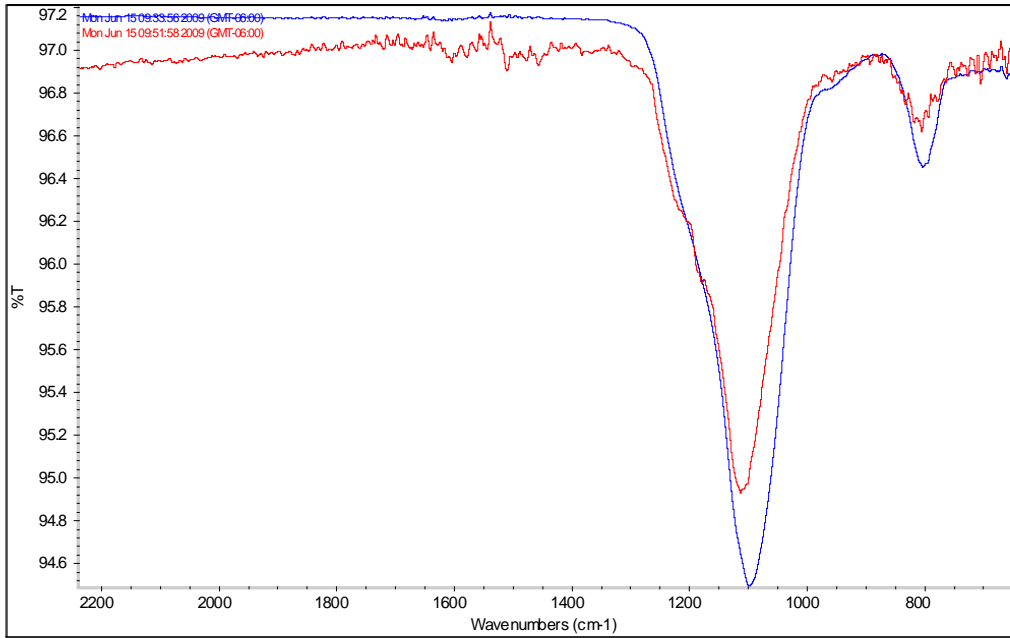


Figure 7-3 FTIR plots for Ludox treated with Mg ions

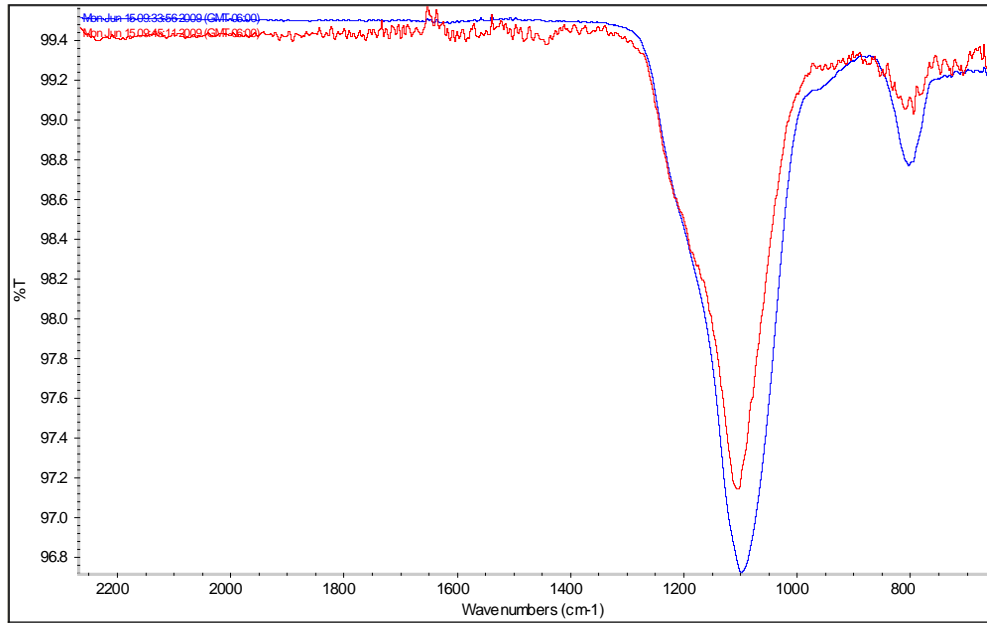


Figure 7-4 FTIR plots for Ludox treated with Sr ions

Chapter 8 Appendix B

8.1 Hydrothermal preparation of silica materials

Ludox was treated with different amounts of reactants at various temperatures. The results for the asphaltene and meta recoveries are listed in Table 8-1.

Table 8-1 Hydrothermal preparations for modification of silica materials.

Sample	Temperature	Reactant type	Reactant(g/100 g packing)
L_1	100	CaO	5
L_2	150	CaO	5
L_3	250	CaO	5
L_4	250	N/A	N/A
L_5	150	MgCl ₂ -6H ₂ O	10
NBrand	150	N/A	N/A
L_7	150	Ba(OH) ₂	10
L_8	80	N/A	N/A

* L refers to Ludox.

8.2 Asphaltene and metal recoveries for different silica materials

Table 8-2 Cumulative asphaltene and metal recoveries for different silica materials

Sample	Reactant type	Cumulative mass recovery%	Cumulative vanadium recovery%
L_1	CaO	26	4.9
L_2	CaO	27	4.9
L_3	CaO	43	38
L_4	N/A	23	8.8
L_5	MgCl ₂ -6H ₂ O	21	1.2
NBrand	N/A	80	63
L_7	Ba(OH) ₂	17	2
L_8	N/A	33	6.2
S_1	N/A	31	5.2
S_2	N/A	36	18

* S_1 refers to separations on sea sand at the flocculation point

* S_2 refers to separations on sea sand at 0.32/0.68 pentane-to-dichloromethane volume ratio.

Chapter 9 Appendix C

9.1 Ni concentrations obtained from ICP analysis

Table 9-1 Ni concentrations obtained from ICP analysis. Different concentrations are obtained using different solvents, chromatography packings and column temperatures.

Packing	Solvent volume ratio	Column temperature(°C)	Ni concentration(ppm)
Sea sand	0.55/0.45 v _{P/D}	25	15.9
Sea sand	0.4/0.6 v _{H/T}	25	0.185
Sea sand	0.4/0.6 v _{H/T}	50	0.195
Untreated	0.55/0.45 v _{P/D}	25	0.570
Mg treated	0.55/0.45 v _{P/D}	25	0.0819
Ca treated	0.55/0.45 v _{P/D}	25	0.0319
Ba treated	0.55/0.45 v _{P/D}	25	0.107
Sr treated	0.55/0.45 v _{P/D}	25	0.0648